Felten, Björn; Felling, Tim; Osinski, Paul; Weber, Christoph

Working Paper

Flow-Based Market Coupling Revised - Part II: Assessing Improved Price Zones in Central Western Europe

HEMF Working Paper, No. 07/2019

Provided in Cooperation with:
University of Duisburg-Essen, Chair for Management Science and Energy Economics

Suggested Citation: Felten, Björn; Felling, Tim; Osinski, Paul; Weber, Christoph (2019) : Flow-Based Market Coupling Revised - Part II: Assessing Improved Price Zones in Central Western Europe, HEMF Working Paper, No. 07/2019, University of Duisburg-Essen, House of Energy Markets & Finance, Essen

This Version is available at:
https://hdl.handle.net/10419/201590

House of Energy Markets & Finance

Flow-Based Market Coupling Revised - Part II: Assessing Improved Price Zones in Central Western Europe

HEMF Working Paper No. 07/2019

by

Tim Felling,
Björn Felten,
Paul Osinski
and
Christoph Weber

June 11, 2019

UNIVERSITÄT DUISBURG ESSEN

Open-Minded

Abstract

Part I of this two-part paper has presented flow-based market coupling (FBMC), the implicit congestion management method used to couple the Central Western European (CWE) electricity markets. It has also introduced a large-scale model framework for FBMC assessments, focusing on modeling the capacity allocation and market clearing processes. The paper at hand lays the focus on the newly developed redispatch model, thereby completing the description of the overall model framework. Furthermore, we provide a case study assessing improved price zone configurations (PZCs) for the extended CWE electricity system. Our case study is motivated by the ineffectiveness of managing congestion of intra-zonal lines described in Part I and by the possibility to reduce their relevance by improved PZCs. The importance of this study is substantiated by the controversial discussions on the currently-existing PZC. Thus, we assess the existing PZC and five novel PZCs determined by a cluster algorithm. Our results show that improved PZCs can reduce redispatch quantities and overall system costs significantly. Notably, we show that substantial improvements are possible when redesigning PZCs while maintaining a similar or slightly increased number of price zones. Moreover, under use of the theoretical considerations in Part I, we explain that increasing the number of price zones may not always increase welfare when using FBMC.

Keywords : price zone, zonal pricing, flow-based market coupling, hierarchical clustering, redispatch

JEL-Classification : D47, L51, Q40, Q41, Q48

Tim Felling
House of Energy Markets and Finance
University of Duisburg-Essen, Germany
tim.felling@uni-due.de

Björn Felten
House of Energy Markets and Finance
University of Duisburg-Essen, Germany
bjoern.felten@uni-due.de

Paul Osinski
(Corresponding Author)
House of Energy Markets and Finance
University of Duisburg-Essen, Germany
paul.osinski@uni-due.de

Christoph Weber
House of Energy Markets and Finance
University of Duisburg-Essen, Germany
christoph.weber@uni-due.de

Contents

List of Figures

List of Tables

Abbreviations

5%-BAU/PZC	Flow-Based Market Coupling
BAU-C	business-as-usual configuration.
CHP	combined heat and power.
CWE(+)	(extended) Central Western Europe(an).
EMCP	electricity market clearing problem.
FB(MC)	flow-based (market coupling).
FRM	flow reliability margin.
GSK	Generation Shift Key
ImpFS	imperfect foresight. Sensitivity as explained in sec. 2.3.
JMM	WILMAR Joint Market Model.
LFC	load flow constraint.
LMP	locational marginal price.
MCC	market clearing costs.
OPF	optimal power flow.
PTDF	power transfer distribution factor.
PZ(C)	price zone (configuration).
RAM	remaining available margin.
RD(C)	redispatch (costs).
SC	system costs.
TSO	transmission system operator.

Nomenclature

$\Delta g_{i,t}^{mbc}$	market-based renewables curtailment at node i.($\delta_u \geq$ 0for $u \in \mathcal{U}^{ext}$, 0 otherwise)
$\Delta g_{u,t}^{+/-}$	pos./neg. RD of unit u in time-step t.
δ_u	power-loss coefficient of unit u.
η_u^{ps}	cycle efficiency of pumped storage unit u.
κ_u	minimum load fraction of unit u.
$\mathcal{U}^{bkp} \subset \mathcal{U}^{disp}$	set of backpressure CHP plants.
$\mathcal{U}^{conv}$	$= \mathcal{U} \setminus \mathcal{U}^{RES,nondisp}$
$\mathcal{U}^{disp}$	set of dispatchable generation units.
$\mathcal{U}^{ext} \subset \mathcal{U}^{disp}$	set of extraction-condensing CHP plants.
$\mathcal{U}^{hydro}$	$= \mathcal{U}^{ps,pump} \cup \mathcal{U}^{hyr}$
$\mathcal{U}^{hyr} \subset \mathcal{U}^{disp}$	set of hydro power plant with reservoirs.
$\mathcal{U}_t^{nonop}$	$= \left\{ u \mid u \in \mathcal{U}^{disp} \wedge g_{u,t} = 0 \right\}$
$\mathcal{U}_t^{noRD,neg}$	$= \mathcal{U} \setminus \mathcal{U}^{RD,neg}$
$\mathcal{U}_t^{noRD,pos}$	$= \mathcal{U} \setminus \mathcal{U}^{RD,pos}$
$\mathcal{U}^{ps,pump} \not\subset \mathcal{U}^{disp}$	set of pumps of pumped storage units.
$\mathcal{U}^{ps,turb} \subset \mathcal{U}^{disp}$	set of turbines of pumped storage units.
$\mathcal{U}^{RD,fast}$	$= \left\{ u \mid u \in \mathcal{U}^{disp} \wedge \tau_u^{lead} \leq 1 \right\} \setminus \mathcal{U}^{bkp}$
$\mathcal{U}_t^{RD,neg}$	$= \mathcal{U}_t^{started} \setminus \mathcal{U}^{bkp}$
$\mathcal{U}_t^{RD,pos}$	$= \mathcal{U}_t^{started} \cup \mathcal{U}^{RD,fast}$
$\mathcal{U}_t^{RD,slow}$	$= \mathcal{U}_t^{started} \setminus \mathcal{U}^{RD,fast} \setminus \mathcal{U}^{bkp}$
$\mathcal{U}^{RES,nondisp}$	set of renewable non-dispatchable units.
$\mathcal{U}_t^{started}$	$= \left\{ u \mid u \in \mathcal{U}^{disp} \wedge g_{u,t} > 0 \right\}$
$\mu_{u,t}^{hyr}$	shadow price of hydro reservoir unit.
$\mu_{u,t}^{ps}$	daily average electricity price.
σ_u	power-to-heat ratio of unit$u \in \left\{ \mathcal{U}^{bkp} \cup \mathcal{U}^{ext} \right\}$
τ_u^{lead}	lead time of unit u
$A_{f,i}$	PTDF of line f for node i.
$b_{i,u}$	unit-to-node allocation.
c^{curt}	reimbursement for renewables curtailment.
C_f	capacity of line f.

$d_{i,t}$	vertical load at node i.
$g_{u,t}$	scheduled dispatch of unit u.
$g_{u,t}^{max}$	available el. capacity of unit u.
$g_{u,t}^{nonsp,+}$	capacity reserved for pos. nonspinning reserve.
$g_{u,t}^{spin,+}$	capacity reserved for pos. spinning reserve.
$g_{u,t}^{spin,-}$	capacity reserved for neg. spinning reserve.
$g_{u,t}^{started}$	started capacity of unit u.
$h_{u,t}^{chp}$	heat extraction of unit u ($h_{u,t}^{chp} \geq 0$ for $u \in \left\{\mathcal{U}^{ext} \cup \mathcal{U}^{bkp}\right\}$, 0 otherwise)
$i \in I$	index/set of nodes of the system.
q_i^{RD}	net electricity surplus at node i after RD.
$V^{(component)}$	price variation in system.
$z \in Z$	index/set of price zones.

1. Introduction

With increasing amounts of variable non-dispatchable electricity generation from renewable sources, the locations of supply and demand of electricity frequently fall apart. Therefore, electricity transmission and congestion management become more and more important for power systems. Their relevance becomes obvious when considering redispatch (RD) amounts and costs in Germany. Both of these quantities have increased by more than 400 % over the last few years [BDEW 2017]. Most of these redispatch measures are taken to avoid overloads of intra-zonal transmission lines (cf. [BNetzA 2017]). Part I [Felten et al. 2019] demonstrates that managing congestion of intra-zonal lines is especially ineffective in FBMC-style zonal market designs. Furthermore, implicit (or explicit) redispatch measures for these lines must already be considered at the capacity allocation stage, introducing further inaccuracies to the market coupling (MC) process.

One way to cope with this challenge could be the implementation of a nodal pricing regime [Hogan 1992] as applied e.g. in parts of North America or New Zealand [Biggar and Hesamzadeh 2014]. However, the European target model builds on coupled yet zonally organized electricity markets. Therefore, a transition to nodal pricing would constitute a fundamental paradigm change and is not likely to occur anytime soon. Having said that, there are further ways to improve congestion management which, at the same time, would be compatible with said target model. Alternative price zone configurations (PZCs), which are geared to frequently congested lines, are one option to reduce intra-zonal congestion while maintaining a zonal market design. In the current PZC, price zones are (mostly) aligned with national borders. This PZC has eventually been questioned [ACER 2014; Löschel et al. 2013], and the European Commission has called for a review of this PZC [European Commision 2015]. However, its results could not be used for a solid and comprehensive assessment of PZCs [Entso-E 2018a] for various reasons [Felten et al. 2019]). Thus, the main research question of this paper is how improved PZCs can contribute to enhancements in congestion management. This question is investigated with special regard to FBMC, as this is the applied MC method in Central Western Europe (CWE). On the one hand, intra-zonal lines take a particular role in FBMC, as their load flow constraints (LFCs) can be considered in FBMC. On the other hand, improved PZCs can re-classify these lines and make them become inter-zonal lines, thereby enhancing the effectiveness of MC. Thus, we investigate improved PZCs for the extended CWE region. The effects in terms of welfare are assessed for almost the entire European continent. For this analysis, we make use of the large-scale modeling framework introduced in [Felten et al. 2019].

The contributions of the paper at hand and its companion are revealed by a review of extant literature. That is existing publications assessing zonal market designs can roughly be clustered in three groups:

1. The first group analyzes stylized (or rather small-scale) zonal systems. Frequently, the benchmark is the nodal market design as first-best solution (e.g. [Ehrenmann and Smeers 2005; Bjørndal and Jörnsten 2001; Bjørndal and Jörnsten 2007; Oggioni and Smeers 2013;

Grimm et al. 2016; Grimm et al. 2017]). Some of these studies [Ehrenmann and Smeers 2005; Bjørndal and Jörnsten 2001; Bjørndal and Jörnsten 2007; Oggioni and Smeers 2013] also assume or determine alternative PZCs for their stylized examples. The companion to this paper [Felten et al. 2019] presents novel zonal-vs.-nodal analyses and is the first of its kind to analyze the effects of all essential FBMC elements. While the use of these stylized examples is a powerful means for understanding/analyzing cause-and-effect relations of MC processes, their value for the quantification of absolute effects, such as welfare changes in real-world systems, is limited [Felten et al. 2019].

2. For this purpose, the second stream of papers encompasses application studies by means of large-scale electricity models. E.g. [Neuhoff et al. 2013; Bertsch et al. 2015; Egerer et al. 2015; Trepper et al. 2015; Finck et al. 2018; Marjanovic et al. 2018; Wyrwoll et al. 2018] apply more sophisticated models for the assessment of the existing PZC. A higher level of sophistication can be attained by replicating market processes in more detail, increasing the regional scope, improving granularity of data, enhancing the representation of technical constraints or other measures. For instance, [Neuhoff et al. 2013; Bertsch et al. 2015; Egerer et al. 2015] contain detailed representations of the grid. In addition, [Bertsch et al. 2015] include transmission grid expansion planning. The market model of [Trepper et al. 2015] contains intertemporal constraints (minimum operation times, minimum downtimes, water reservoir filling levels, etc.), a combined modeling of the heating market and other technical restrictions, but only a simplified representation of the grid. These studies are usually based on the existing PZC. E.g. [Egerer et al. 2015] and [Trepper et al. 2015] assess the effects of splitting the existing German-Austrian price zone whereas [Neuhoff et al. 2013] and [Bertsch et al. 2015] model the existing PZC and contrast the resulting market outcomes with those of a nodal market design.[1] In contrast to the previously named studies, FBMC procedures are considered in recent works of [Finck et al. 2018; Marjanovic et al. 2018; Wyrwoll et al. 2018]. Therein [Marjanovic et al. 2018; Finck et al. 2018] investigate the effects of extending FBMC region to Central Eastern Europe, while [Wyrwoll et al. 2018] present effects of different FBMC parametrizations. Notably, none of the latter studies investigates improved PZCs. In turn, the large-scale model framework used within this paper considers FBMC as well and, at the same time, is applied to assess improved PZCs.[2] Thus, we do not limit the assessment to the existing PZC (or a breakdown of it) and thereby contribute significantly to the above mentioned European Commission request for a more efficient PZC [European Commision 2015]. Linking the large-scale model results to the analyses from Part I [Felten et al. 2019] yields the possibility of in-depth interpretation of results, which makes our papers unique.

[1] Despite having assigned these studies to the group of large-scale applications, it should be noted that some of these studies only assess a limited set of hours or do not consider important technical constraints.

[2] More precisely, we model the combination of FBMC (as being applied in CWE) and NTC-based MC (as applied for the remaining European markets)

3. The third stream of papers departs from basing the assessments on the existing PZC (e.g. [Burstedde 2012; Breuer 2014; Felling and Weber 2018; Imran et al. 2008; Van den Bergh et al. 2016; Sarfati et al. 2015; Kłos et al. 2014]). They address the question of how to determine new price zones, what we henceforth refer to as long-term price zone reconfiguration process. Therein, the focus is often laid on defining a set of criteria or developing an algorithm for grouping nodes to zones. These algorithms use information at the level of (aggregated) grid nodes/transmission lines, i.e. locational marginal prices (LMPs) in [Burstedde 2012; Imran et al. 2008; Breuer 2014; Felling and Weber 2018] or power transfer distribution factors (PTDFs) [Sarfati et al. 2015; Kłos et al. 2014; Van den Bergh et al. 2016]. Usually, applied models either comprise a detailed grid and a simplified market model or vice versa. Thus, real-world complexities are simplified in either one dimension. The paper at hand does not make such compromise. Making use of specialized and proven tools, enhancing them and combining them in the developed model framework allows us to reproduce all stages of the MC process (i.e. capacity allocation, market clearing and redispatch).

In summary, the paper at hand contributes by combining the mentioned streams of studies. Thereby, typical limitations of existing studies in this field are overcome and more profound and realistic assessments are performed. The results comprise not only an in-depth analysis of technical and socio-economic impacts of different PZCs (e.g. changes in dispatch schedules, redispatch amounts, shifts of generation between PZCs, changes in welfare and related redistributive effects). They also show how some of the shortcomings of FBMC can eventually be overcome by improved PZCs whilst the relevance of others is increased.
The remainder of this paper is organized as follows. Sec. 2 outlines the developed methodology. This includes the process of identifying improved PZCs. Moreover, the modeling of the stages of the MC process is explained. While the D-2 and the D-1 stage have been explained in detail in Part I, we herein focus on the formal description of the model of the D stage, i.e. the redispatch model. Subsequently, Sec. 3 presents the case description. Sec. 4 continues with exhibiting the relevant results and sec. 5 draws the main conclusions.

2. Methodology

2.1. Overall Methodology

Fig. 1 provides an overview of the used methodology. The assessment starts with a (long-term) price zone reconfiguration process. Effectively, this encompasses the methodology of determining price zone delimitations. Therefore, we apply the hierarchical cluster algorithm developed in [Felling and Weber 2018]. Thus, we only shortly summarize its main operations and functions in sec. 2.2. This process yields a sequence of PZCs with different numbers of zones, out of which distinct PZCs are selected. Each PZC is defined by a node-to-zone allocation matrix. By use of this matrix, the input data are structured and the models are configured [Felten et al. 2019]. For each PZC, the stages of the electricity market are simulated; i.e. starting with the first stage two days before delivery (D-2) at which the FBMC parameters are determined, followed by the day-ahead market (D-1). As these two stages have been discussed in detail in the companion to this paper [Felten et al. 2019], we focus on the explanation of case-specific model settings in sec. 2.3 and 2.4. In turn, the formal description of the real-time (D) stage has not been provided in [Felten et al. 2019]. Therefore, the redispatch (RD) model is presented in detail in sec. 2.5. After having simulated the three stages for each PZC, an important step is constituted by individual and combined assessments of the model outcomes. Therefore, the most relevant evaluating operations are described in sec. 2.6.

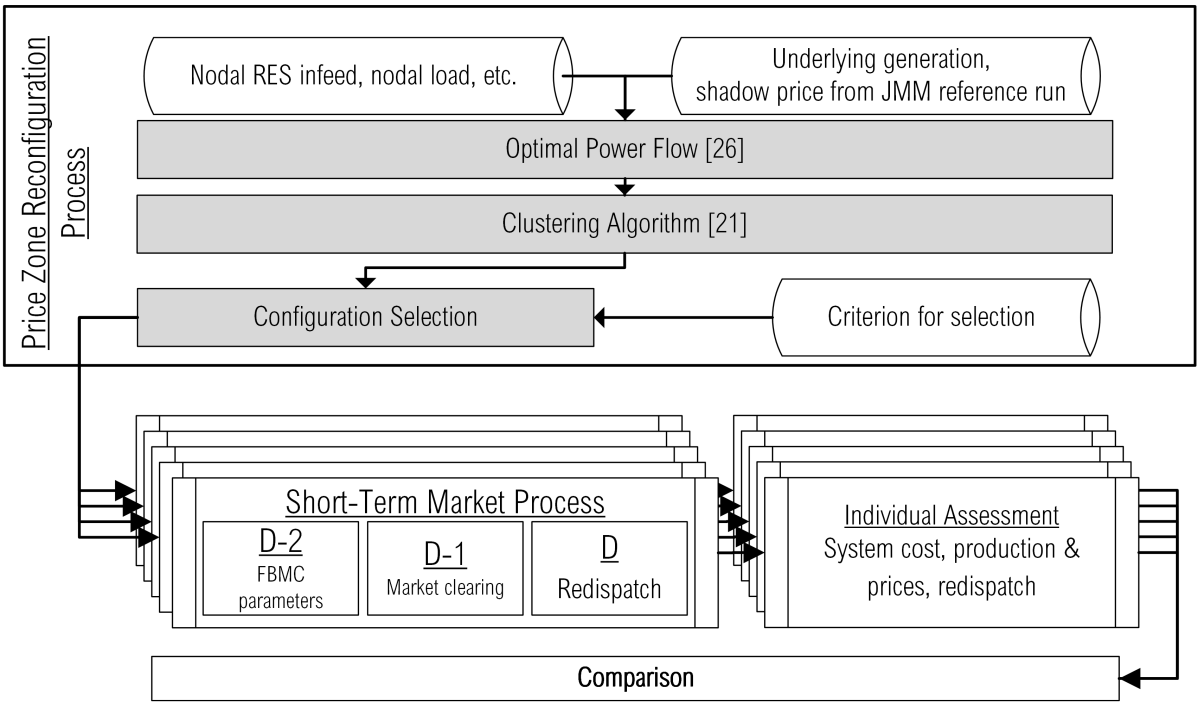

Figure 1: Schematic illustration of the price zone reconfiguration process and its link to modeling and assessing short-term market processes.

2.2. Price Zone Reconfiguration Process

This section describes the method of identifying new PZCs as alternatives to the existing configuration. We apply the hierarchical cluster algorithm developed in [Felling and Weber 2018] and therefore only summarize briefly the algorithm's main operations.
The algorithm clusters nodes to zones based on similarity of LMPs. Similarity of LMPs at two nodes implies that sufficient transmission capacity is available between these nodes. Hence, when determining possible price zones, nodes should be aggregated first where LMPs are most similar. Due to the hierarchical structure of the algorithm, it starts with the configuration in which every node corresponds to exactly one zone (nodal set-up) and ends when all nodes are grouped to one zone. In each stage of the clustering procedure, two zones are aggregated following a specific merging criterion being the least increase in price variation within zones V^{within}. This entails PZCs with individual zones having prices as homogeneous as possible and being delimited by lines that tend to be congested. In [Felling and Weber 2018], the authors show that the total price variation in a system V can be decomposed into a variation between and within price zones ($V^{between}$ and V^{within} respectively). Thus, in a nodal set-up (first iteration), the total price variation in the system, relative to V, is found between zones ($V^{between}/V = 100\%$) while in the last iteration, when all nodes form one zone, all price variations are within this zone ($V^{within}/V = 100\%$). The required LMPs are computed by the DC-lossless approximation of the optimal power flow (OPF) calculation based on [Zimmermann et al. 2011] in a first step and then serve as input data for the clustering algorithm.

2.3. D-2 Stage: Capacity Allocation

The formal methodology of determining FBMC parameters, i.e. remaining available margins (RAMs), zonal PTDFs and the applied methods of involved transmission system operators (TSOs) for the calculation of generation shift keys (GSKs), has been described in Part I [Felten et al. 2019]. According to [Dierstein 2017], one of the most frequently applied GSK procedures is the GSK calculation proportional to installed dispatchable power plant capacities. In order to use one consistent GSK procedure for all FBMC regions, we use this procedure for all FBMC regions. With regard to the base case estimation, the selection of considered intra-zonal line flow constraints (LFCs) and the choice of flow reliability margins (FRMs), we perform sensitivity calculations. Subsequently, we first explain the settings of the assessed reference case. Thereafter, the sensitivities are explained. In general, the sensitivities are defined by changing exactly one feature of the reference case. All other features remain unchanged.

2.3.1. Reference case

For the reference case, we use a base case that is characterized by perfect foresight of the theoretically possible renewable generation[3], i.e. there is no deviation between the renewables forecast two days ahead of delivery (D-2) and its actual realization at the day of delivery (D). In terms of considered LFCs, the reference case does not consider any intra-zonal lines. Furthermore, in the reference case and all sensitivities, FRMs are based on a percentage value of the line capacity. For the reference case, this percentage value is set to 12%.

2.3.2. Base case sensitivity (ImpFS)

We investigate the influence of forecast errors of renewables generation by considering imperfect information at the D-2 stage. The relative forecast errors are calibrated to historic forecast errors of the respective TSOs for the year 2017 [Entso-E 2018b]. These relative forecast errors are then applied to the used infeed time series yielding absolute forecast deviations. For the market clearing, the actual realizations are used.

2.3.3. Intra-zonal line sensitivity 1 (5%-PZC)

In Part I [Felten et al. 2019], we have explained that intra-zonal lines are considered significant if any zone-to-zone PTDF has an absolute value greater than 0.05 [Amprion et al. 2014]. In this sensitivity, we apply this criterion for each PZC. Thus, we calculate the zonal PTDFs and all zone-to-zone PTDFs for each PZC. If the threshold of 0.05 is exceeded at least once for an intra-zonal line, the corresponding LFCs are considered. Henceforth, we refer to this sensitivity as 5%-PZC.

2.3.4. Intra-zonal line sensitivity 2 (5%-BAU)

For calculating whether an intra-zonal line exceeds the above-described 5% threshold or not, the only input parameters are (nodal) PTDFs and GSKs. Notably, other factors like the levels of net exports of zones and line capacities are no input parameters to the calculation. However, latter factors were implicitly considered in the process of establishing the 5% threshold, as the TSOs determined it by testing various alternative threshold values [Amprion et al. 2014]. This was done under consideration of the given PZC, i.e. under use of corresponding net export levels and line capacities. When considering alternative PZCs, the standard deviation of zonal PTDFs increases. As the worst-case zone-to-zone PTDF is subject to assessment, using the 5% threshold tends to result in a high number of intra-zonal constraints even though critical

[3]The term "theoretically possible" refers to the renewables infeed that is possible at plant level. That is to say the value does not consider any restrictions that may be imposed by the grid.

zone-to-zone trades tend to be smaller and, thus, the line capacities can be expected to be sufficient in many situations. In order to avoid this bias, we define the sensitivity 5%-BAU. In this sensitivity, the LFCs of the set union of the lines considered for the business-as-usual configuration (BAU-C) and the inter-zonal lines of the regarded PZC are considered. Thus, the set of intra-zonal lines is not empty (as in the reference case) but, at the same time, not as large as in 5%-PZC.

2.3.5. FRM sensitivity

In this sensitivity, we do not keep the FRM values constant anymore. Instead, we decrease the percentage value for FRM calculation reciprocally to the number of zones. In order to attain 12% for the BAU-C, the FRM equals 60% divided by the number of zones. That yields 12% for the BAU-C and, for instance, 1.2% for a PZC with 50 zones.

2.4. D-1 Stage: Market Clearing

For modeling the market clearing, the WILMAR Joint Market Model (JMM) is used. This detailed scheduling model is described in detail in [Meibom et al. 2006]. The model has been enhanced to simulate FBMC and restrictions of combined heat and power (CHP) plants that result from heat extraction (c.f. [Felten et al. 2019; Felten 2016; Felten et al. 2017]). Some of its applications are presented in [Tuohy et al. 2009; Meibom et al. 2011; Trepper et al. 2015]. Since the JMM depicts almost the complete European electricity market (continental Europe plus Scandinavia, UK and Ireland and excl. member states of the former Soviet Union), the linear deterministic program version is chosen in this case study in order to keep calculation times manageable. This especially entails that generators are grouped to so-called unit groups (i.e. groups of units of same technological type, using the same fuel, having similar ages and being located in the same PZ). Using the deterministic set-up entails that power plant operators are modeled to have perfect knowledge of renewables-based generation and power plant availabilities at day-ahead bidding stage (D-1 stage). Such perfect knowledge basically represents an upper bound for the bidding performance of the power plant operator and, having inelastic demand, for the welfare achievable through the market clearing process under the given constraints. It further entails that day-ahead and intraday clearing results are almost identical. Hence, we refer to the results of both (day-ahead and intraday) as scheduled dispatch or market outcomes, even though, formally, intraday market clearing would correspond to the D stage of the market. It is important to note that the deterministic setting of the JMM only concerns the bidding and market clearing process under use of given constraints. The exchange capacities that are allocated to the market at the D-2 stage are not deterministic. As explained in Part I [Felten et al. 2019], the FBMC procedures can yield inaccurate LFCs in various ways and, therefore, constraints used in the market clearing are not perfect. This also constitutes one focus area

of our case study in sec. 3 to 5. It should also be noted that the model assumes that market participants bid truthfully, not trying to profit from potentially predictable price differences between the D-1 and D stage. In CWE, RD is highly regulated and essentially cost based and therefore incentives for strategic bidding are small.

2.5. D-Stage: Redispatch

In order to model the processes at the D stage, we have developed a novel redispatch (RD) model. The basic principle of RD can be described as follows. Once the markets have been cleared, dispatch schedules (and updated renewables forecasts) are known to the TSOs. From these schedules, corresponding line loadings can be calculated. If line overloads result from the scheduled dispatch, TSOs must take measures to assure a safe and reliable grid operation. In this case, the by far most frequent measure is the interference of the TSO in the dispatch schedule of power plants, i.e. RD (including renewables curtailment)[BNetzA 2017]. Thus, the responsible TSO identifies adjustments to power plant dispatch that reduce critical line loadings and, in sum, avoid overloads. Interference into the dispatch schedule also impacts the economics of power plant operators. Therefore, generators are reimbursed or need to pass on saved operational costs. This is explained as follows:

1. Positive RD $\Delta g^{+}_{u,t} > 0$: Increasing the generation of power plants downstream of an overloaded line reduces its critical loading. For ramping up and operating these plants, additional costs are incurred by power plant operators, and these need to be reimbursed by the responsible TSO. Apart from the variable costs of steady-state operation $c_{u,t}$, cost of start-up fuel, start-up depreciation costs, etc. exist. As only additional costs are reimbursed to instructed power plant operators, the contribution margins of this operation is 0. Thus, overall producer rents remain unchanged from those attained on the markets. From a system perspective, reimbursed costs add to the costs determined by the market clearing.

2. Negative RD $\Delta g^{-}_{u,t} > 0$: Generation of power plants upstream of an overloaded line aggravates its critical loading. When these generators are ordered to reduce generation, they remain with the revenues from previous power sales. However, they need to pay the saved variable costs $c_{u,t}$ minus additional cycling and other costs to the TSO. In essence, generators should remain with their contribution margins which they would have attained through the scheduled dispatch. Thus, also in case of negative RD, producer rents are not changed. From a system perspective, only the amount payable from the power plant operator to the TSO reduces RD costs. In case of renewables curtailment, the economics are different in one major aspect. The curtailment causes a reduction of revenues which mostly stems from lost payments according to renewables support schemes and, therefore, renewables curtailment is usually more costly than RD of non-renewable power plants.

The German legislation on this topic [Oberlandesgericht Düsseldorf 2015] reveals that RD reimbursement and chargeable costs have numerous elements (e.g. opportunity revenues from sales at different markets, lost entitlement to regulatory payments, cost of alternative heat supply, etc.) and that special arrangements are allowed. The exact reimbursement/cost figures are not public. Therefore, in the RD model, we use a term γ_u to model the costs that come in addition to $c_{u,t}$. We set γ_u to 0.2, i.e. reimbursable costs for positive RD are 20% higher than $c_{u,t}$ and chargeable costs for negative RD are 20% lower than $c_{u,t}$. A rough estimate like this helps to overcome non-existence of publically available actual cost data. However, a factor like γ_u has influence on model results. In order to assess the sensitivity of our model to γ_u, we perform a sensitivity analysis in app. A.
In line with the previous statements, the optimization problem is stated in eq. (1) to (13). Precedent to this, we define the used sets and variables and explain the input parameters and the reasoning behind the objective function and restrictions.

2.5.1. RD objective

The objective of the responsible TSOs (and the developed RD model) is to avoid line overloads while causing least additional system costs possible. Thus, the scheduled dispatch $g_{u,t}$ of all hours of the year T is handed over from the JMM to the grid model. A power flow calculation is performed in MATPOWER [Zimmermann et al. 2011] in order to detect line overloads. Subsequently, RD amounts are determined using the cost-minimizing objective in eq. (1) for all hours with (scheduled) overload situations T^{RD}. Therein, $\Delta g_{u,t}^{+/-}$ denote positive/negative RD amounts, $c_{u,t}^{+/-}$ the corresponding specific reimbursable/chargeable costs (item (1) and (2)). We explain the optimization problem in detail in sec. 2.5.4 below. For now, it is sufficient to note that the formulated RD problem can be understood as cost-based RD, as it is performed in actual practice (cf. [Frontier Economics and Consentec 2008]).

2.5.2. Sets of power plant units

It is important to distinguish between different power plants. The distinctions are made in terms of technical availability, applicability of regulatory regimes, operational states (according to the scheduled dispatch) and in terms of combinations of aforementioned aspects. As they generally depend on the operational state as per dispatch schedule, some unit sets are time dependent (index t). All defined sets are listed in the nomenclature.

2.5.3. Parameters

We utilize the market outcome determined in the JMM as input parameters for the RD model. This comprises not only the scheduled dispatch but also the outcome of the different reserve

markets and the shadow prices of hydro power plants. Furthermore, the scheduled heat extractions $h_{u,t}^{chp}$ of CHP plants are considered, as they restrict the redispatch ability further. $h_{u,t}^{chp}$ is the output of the CHP tool described in [Felten et al. 2017]. One parameter that should be briefly explained is $g_{u,t}^{started}$. In the JMM, it has several purposes (cf. [Meibom et al. 2006]). The most important one is to model intertemporal constraints of unit groups, such as shutdown or operating periods, that have to last for a minimum number of consecutive hours. Thus, for the RD model, only part of the unit group is in operation (started) and only, in case of slow units, this started capacity is available for positive RD. At the same time, the technical minimum load is also determined by means of $g_{u,t}^{started}$ (cf. eq. 10).

2.5.4. RD optimization problem

With the above definitions, the optimization problem in eq. (1) to (13) can be formulated as follows:

$$min_{\Delta g_{u,t}^{+},\Delta g_{u,t}^{-}} \sum_{t\in T^{RD}} \sum_{u\in\mathcal{U}} (c_{u,t}^{+}\Delta g_{u,t}^{+} - (c_{u,t}^{-} - c_{t}^{max})\Delta g_{u,t}^{-}) \tag{1}$$

$s.t.$

$$\sum_{i\in I} A_{f,i} q_{i,t}^{RD} \leq C_f \qquad \forall\ f\in F,\ t\in T^{RD} \tag{2}$$

$$-\sum_{i\in I} A_{f,i} q_{i,t}^{RD} \leq C_f \qquad \forall\ f\in F,\ t\in T^{RD} \tag{3}$$

$$q_{i,t}^{RD} = \sum_{u\in U} b_{u,i}(g_{u,t} + \Delta g_{u,t}^{+} - \Delta g_{u,t}^{-}) - d_i - \Delta g_{i,t}^{mbc} \qquad \forall\ i\in I,\ t\in T^{RD} \tag{4}$$

$$\Delta g_{u,t}^{+} \leq g_{u,t}^{started} - g_{u,t}^{spin,+} - g_{u,t}^{nonsp,+} - \delta_u h_{u,t}^{chp} - g_{u,t} \qquad \forall\ t\in T^{RD},\ u\in\mathcal{U}^{RD,slow} \tag{5}$$

$$\Delta g_{u,t}^{+} \leq g_{u,t}^{max} - g_{u,t}^{spin,+} - g_{u,t}^{nonsp,+} - \delta_u h_{u,t}^{chp} - g_{u,t} \qquad \forall\ t\in T^{RD},\ u\in\mathcal{U}^{RD,fast} \tag{6}$$

$$\Delta g_{u,t}^{+} \leq g_{u,t} - g_{u,t}^{spin,+} - g_{u,t}^{nonsp,+} \qquad \forall\ t\in T^{RD},\ u\in\mathcal{U}^{ps,pump} \tag{7}$$

$$\Delta g_{u,t}^{+} = 0 \qquad \forall\ t\in T^{RD},\ u\in\mathcal{U}^{noRD,pos} \tag{8}$$

$$\Delta g_{u,t}^{-} \leq g_{u,t} - \sigma_u h_{u,t}^{chp} - g^{spin,-} \qquad \forall\ t\ \in T^{RD},\ u\in\mathcal{U}^{RD,neg} \tag{9}$$

$$\Delta g_{u,t}^{-} \leq g_{u,t} - \kappa_u g_{u,t}^{started} - \delta_u h_{u,t}^{chp} - g^{spin,-} \qquad \forall\ t\ \in T^{RD},\ u\in\mathcal{U}^{RD,neg} \tag{10}$$

$$\Delta g_{u,t}^{-} \leq g_{u,t}^{max} - g_{u,t}^{spin,-} - g_{u,t}^{nonsp,-} \qquad \forall\ t\in T^{RD},\ u\in\mathcal{U}^{ps,pump} \tag{11}$$

$$\Delta g_{u,t}^{-} = 0 \qquad \forall\ t\in T^{RD},\ u\in\mathcal{U}^{noRD,neg} \tag{12}$$

$$\sum_{u\in U} \Delta g_{u,t}^{+} = \sum_{u\in U} \Delta g_{u,t}^{-} \qquad \forall\ t\in T^{RD} \tag{13}$$

The optimization problem is solved in MATPOWER under use of the DC-OPF function (cf. [Zimmermann et al. 2011]).[4] Apart from the non-negative decision variables for the positive and negative RD amounts $\Delta g_{u,t}^{+/-}$, only the nodal net export after RD q_i^{RD} constitutes a (dependent)

[4]For the mathematical description, we neglect variables that can be used for grid topology changes, as we do not consider such changes in this paper (except phase shifting transformers). Furthermore, we use the PTDF

variable. All other symbols in eq. (1) to (18) denote parameters to the RD problem. Eq. (2) and (3) describe the physical LFCs as explained in Part I [Felten et al. 2019]. Eq. 4 describes the nodal net exports after RD. Eq. (5) to (8) constitute the constraints for positive RD applicable to distinctive sets of units. Eq. (9) to (12) are the analogous constraints for negative RD. Eq. (13) assures the energy balance (cf. [Felten et al. 2019]). In addition to the aforementioned cost terms, the objective function contains a further term c_t^{max}. Otherwise, a straightforward cost-minimizing problem would perform a re-optimization of the scheduled dispatch. That is, in some situations, the grid model would identify nodal dispatch improvements in order to reduce costs (in addition to relieving anticipated overloads). The reason is that the JMM models technical restrictions on power plant level in much more detail. For instance, intertemporal constraints can cause power plants to operate even though these power plants may temporarily not be in the money. These constraints are real-world restrictions which are represented in the JMM in more detailed than in the RD model (cf. [Meibom et al. 2006]). Another example for possible re-optimization is given by LFCs in the market clearing. Part I [Felten et al. 2019] has demonstrated that the market clearing problem in an FBMC zonal market design can be subject to unnecessarily restrictive LFCs and only disposes of limited means to manage intra-zonal congestion. This can lead to suboptimal market outcomes. As the grid model considers the exact LFCs and can manage intra-zonal congestion on nodal level, an OPF tends to improve grid utilization and congestion management. As RD is not executed for cost-minimizing purposes, provisions need to be made to avoid such re-optimization of market outcomes in an OPF. We do this by including c_t^{max} in the objective function (eq. (1)). c_t^{max} denotes the variable costs of the most expensive generator. Thus, for purposes of the optimization, negative RD is modelled to cause additional costs at a marginal value of $c_t^{max} - c_{u,t}^{-}$, and these costs have the reverse order of the variable costs of the generators. Thereby, the variable costs of power plants derive as follows. We express the marginal costs of thermal generation as a linearization of the total cost increase $\Delta C_{u,t}$ relative to the generation increase $\Delta g_{u,t}$ (eq. (14)). This yields different costs for plants starting from either zero-generation or from minimum part load. Hence, the effect of low part load efficiencies is considered. With regard to variable costs of pumped storage (eq. 16 and 17), we use the opportunity cost rationale described in [Steffen and Weber 2016].

$$c_{u,t} = \frac{\Delta C_{u,t}}{\Delta g_{u,t}} \qquad \forall\, u \in \{\mathcal{U}^{disp} \setminus \mathcal{U}^{hydro}\} \tag{14}$$

$$c_{u,t} = \mu_{u,t}^{hyr} \qquad \forall\, u \in \mathcal{U}^{hyr} \tag{15}$$

$$c_{u,t} = \mu_{u,t}^{ps} + \mu_{u,t}^{ps} \frac{1-\eta_u^{ps}}{1+\eta_u^{ps}} \qquad \forall\, u \in \mathcal{U}^{ps,turb} \tag{16}$$

$$c_{u,t} = \mu_{u,t}^{ps} - \mu_{u,t}^{ps} \frac{1-\eta_u^{ps}}{1+\eta_u^{ps}} \qquad \forall\, u \in \mathcal{U}^{ps,pump} \tag{17}$$

$$c_{u,t} = c^{curt} \qquad \forall\, u \in \mathcal{U}^{res} \tag{18}$$

notation because it is analogue to Part I [Felten et al. 2019] and, under used simplifications, mathematically equivalent to the formulation with voltage angles.

2.6. Main Assessments of Model Outcomes

The relevant results can be broken down into market outcomes and RD results. The corresponding evaluation steps are explained as follows.

Market results The JMM delivers results on all relevant market outcomes, i.e. electric and thermal generation by fuel and by unit group, electricity prices, exchanges, generation costs, producer and consumer rents, etc. In this study, we focus on three main issues.
Firstly, we are interested in the welfare changes. I.e. we investigate changes of the total operational costs as per scheduled dispatch. Hereinafter, we refer to these costs as market clearing costs (MCC). These costs comprise all variable costs of generators (e.g. fuel and CO_2 costs, variable operation and maintenance costs). We adjust this term by the value of final water reservoir filling volumes. As final filling levels of reservoirs may vary for different PZCs, this decreases/increases the opportunity to achieve future revenues. The valuation is made at the final opportunity costs of water in the corresponding PZ of the reference configuration.[5] Decreases in MCC after the water value adjustment[6] correspond to welfare increases as per market clearing. These results are reported in sec. 4.1. Second, as welfare changes are not equally distributed to involved parties, i.e. consumers, producers and network owners, these redistributive effects constitute a major issue of alternative PZCs. Therefore, the changes in consumer, producer and congestion rents at country level are analyzed. Thus, we map the rents of PZs back to countries, by weighting consumer rent and congestion rent by demand and by adding up contribution margins of plants. The result of interest is the scheduled dispatch. Each unit group's schedule is taken and disaggregated to units, which serves as input for the RD model (cf. sec. 2.5) and for further analyses (cf. sec. 4.2.1).

Redispatch results .The assessment of amounts of the RD model is straightforward. Values for $\Delta g_{u,t}^{+/-}$ result from the optimization problem presented in sec. 2.5.4 and can be broken down by fuel, node, time, etc. Furthermore, scheduled line overloads and free capacities on lines are a result of the initial power flow calculations of the RD model. In terms of assessment of RD costs (RDC), there is one relevant aspect. In the objective function of the RD model (eq. 1), we have used c_t^{max} to avoid re-optimization of market outcomes. However, the term $\sum_{t\in T^{RD}} \sum_{u\in\mathcal{U}} c_t^{max} g_{u,t}^{-}$ serves for OPF purposes only. Thus, we use the objective value of the RD problem reduced by $\sum_{t\in T^{RD}} \sum_{u\in\mathcal{U}} c_t^{max} g_{u,t}^{-}$ for the purpose of RDC assessment. Notably, the factor γ_u is an important parameter when determining RDC. Thus we provide a sensitivity analysis for different γ_u values in app. A.

[5] As the opportunity for electricity sales from hydro generation in the Nordic countries is significantly reduced in all improved PZCs (cf. sec. 4.2.1), we use the final water value of a PZC with a medium number of PZs (8-ImpC) for the adjustment.
[6] For brevity, we do not explicitly state the water value adjustment henceforth. However, it always is included.

3. Case Study Data

In this section, we describe the most relevant data assumptions for our case study. Table 1 gives an overview of the relevant power plant data assumptions. The case study is performed for the year 2020. In the following, the corresponding sources are explained further. The power plant data are based on the Platts power plant database [Platts 2018]. The data have been updated continuously and enhanced by further input data (e.g. agency data such as [BNetzA 2018] or TSO data such as [50Hertz et al. 2014]) and plant-specific research mainly relying on plant owners' web presence and press releases. Future commissioning and decommissioning dates are assumed as per actual announcements and official plannings (e.g. [50Hertz et al. 2014]). Aggregate installed capacities for conventional power plants and renewables-based generators (cf. table 1) are adjusted to match the trend scenario of Entso-E's System Outlook and Adequacy Forecast [Entso-E 2015b].
The time series data are generally based on the year 2012, while absolute annual values are

Table 1: Overview of capacities and RES assumptions for the year 2020.

	AT	BE	CH	DE	FR	LU	NL
Installed Capacity [GW]							
Biomass	0.12	1.71	0	6.39	0.97	0	0.49
Hard coal	0.35	0.02	0	27.63	2.81	0	4.75
Hydro	10.58	0.1	12.11	3.95	21.11	0.04	0.04
Lignite	0	0	0	17.05	0	0	0
Natural gas	5.12	5.65	0.25	25.88	12.4	0.44	19.57
Nuclear	0	5.06	2.80	8.11	63.00	0	0.49
Other	0.16	0.11	0.31	6.35	3.18	0	0.18
Pump storage	4.73	1.44	3.13	7.78	4.09	0	0
Yearly Production [TWh]							
Solar	2.4	3.6	1.7	42.9	10.9	0.1	5.6
Wind offshore	0	7.4	0	26.8	4.2	0	3.9
Wind onshore	9.1	6.0	0.2	93.1	28.6	0.2	10.0

projected to the year 2020. National RES profiles for 2012 are used as published by the respective TSOs, while demand profiles for 2012 are taken from Entso-E (cf. [Entso-E 2015a; Entso-E 2016]). The yearly electricity demand is assumed to stay constant over the years and is taken from the IEA Electricity Information [International Energy Agency 2014]. Hourly renewables-based infeed and demand time series at nodal level are calculated as described in Part I [Felten et al. 2019]. The regional distribution of renewables is thereby based on a broad range of publications from national ministries, offices and TSOs.
We use quotations for fuel and CO_2 futures at the European Electricity Exchange [Energate 2018]; i.e. three-month-average notations of traded 2020 (or latest available[7]) futures product for coal, natural gas, fuel oil and light oil as well as for CO_2 prices. The price for lignite is based on values used in the German Grid Development Plan [50Hertz et al. 2014].

[7]The notations were taken at the time when setting up the case study data, i.e. April to June 2015. In case trade of a 2020 futures product had not started at this time, we used the latest available futures product.

While market simulations comprise almost entire Europe (see more details in sec. 2.4), in order to cope with interdependences across Europe, the transmission grid is modelled for the extended CWE area (CWE+, i.e. Austria, Belgium, France, Germany, Luxembourg, the Netherlands and Switzerland) including the 220- and 380-kV voltage levels. In parts of Germany, 110-kV transformers are also modelled. The grid model is based on publicly available data (among others, static TSO grid models as under [APG 2017; RTE France 2015; TenneT TSO GmbH 2015]). For the analysis, we use the electricity grid of the year 2016 as a base line (start of the case set-up). This is equivalent to assuming delays in grid extension of up to 4 years. In total, over 2,200 nodes, 3,600 branches and 600 transformers are modelled.

4. Results

This section presents and discusses key findings of our approach. First, we present the results of the cluster algorithm, i.e. the improved PZCs (sec. 4.1). Subsequently, we investigate the reference case, exemplary highlight the impact of a specific reconfiguration on market RD results. The same section (sec. 4.2) includes a discussion on the distribution and the course of welfare changes (sec. 4.2.3 and 4.2.4). Thereafter, the investigated sensitivities conclude this section (sec. 4.3).

4.1. Price Zone Reconfiguration

The hierarchical clustering algorithm yields 2226 PZCs, what corresponds to one PZC for each merge of zones ($card(I) - 1 = 2226$). As explained in sec. 2.2, the objective function of the algorithm is to minimize V^{within} Thus, we use V^{within}/V as selection criterion for PZCs for a given number of PZs. Fig. 2 shows how the normalized within-zone variation decreases with the number of PZs. Also threshold values are indicated which are used to select PZCs for further investigations. The thresholds of 15%, 10%, 5% and 2.5% respectively correspond to PZCs with

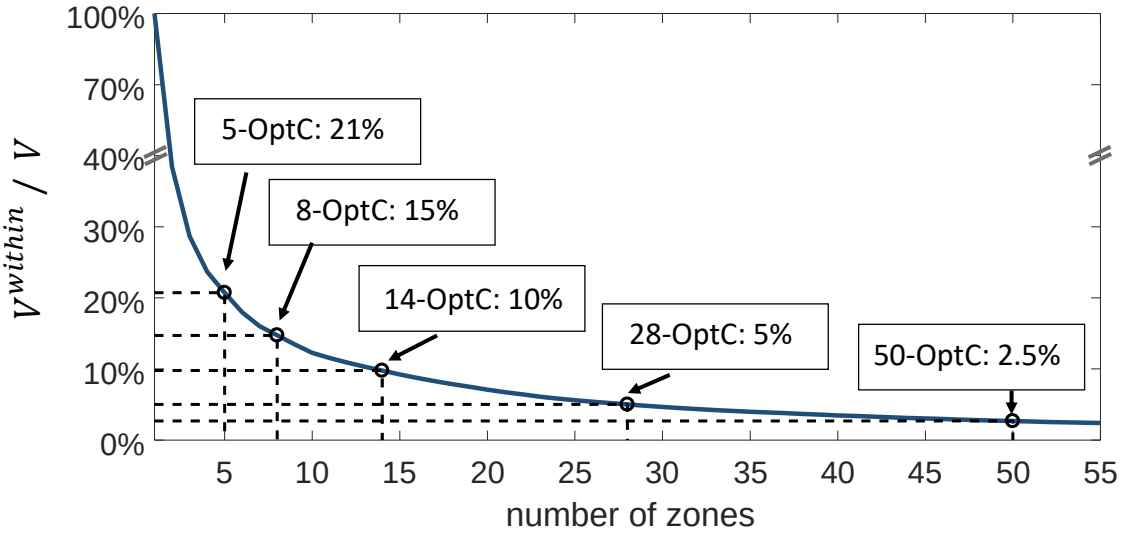

Figure 2: Normalized values for V^{within} as a function of the number of zones.

8, 14, 28 and 50 zones. In addition, we assess the existing PZC with 5 PZs, which we call business-as-usual configuration (BAU-C) henceforth. As explained in sec. 2.2, we also consider an improved 5-zone configuration obtained from the clustering algorithm for our assessment. The improved PZCs are denoted 5-ImpC, 8-ImpC and so forth. Fig. 5 to 8 illustrate the geographical scope of the PZs for all assessed PZCs.

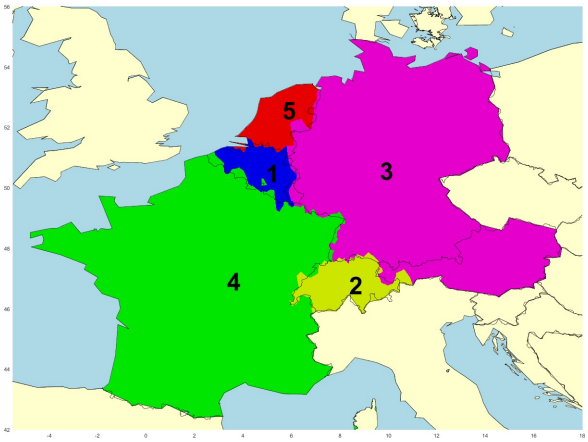

Figure 3: BAU-C.

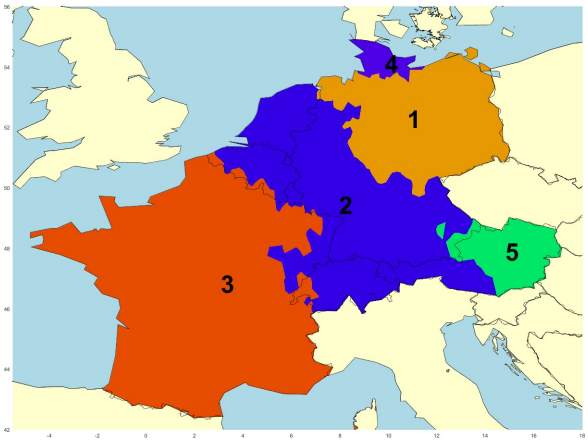

Figure 4: 5-ImpC.

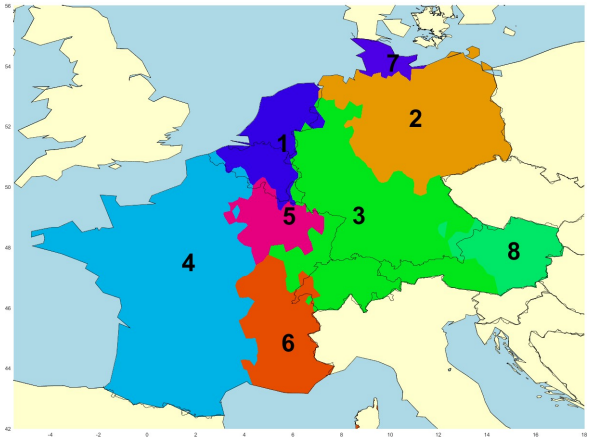

Figure 5: 8-ImpC.

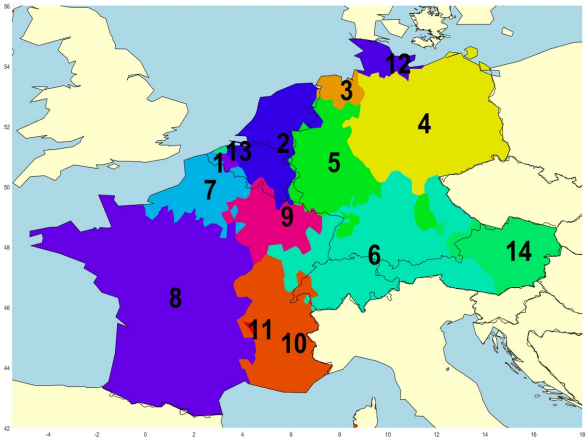

Figure 6: 14-ImpC.

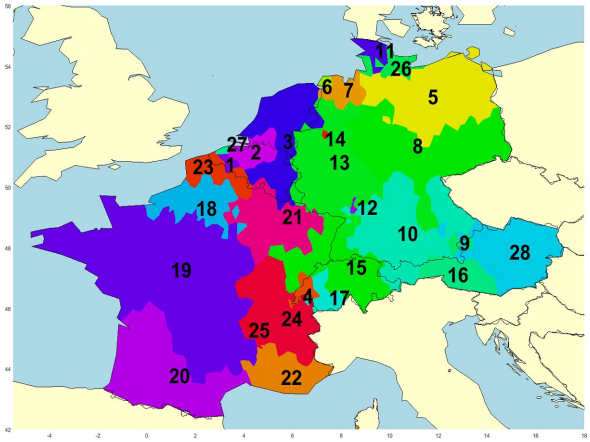

Figure 7: 28-ImpC.

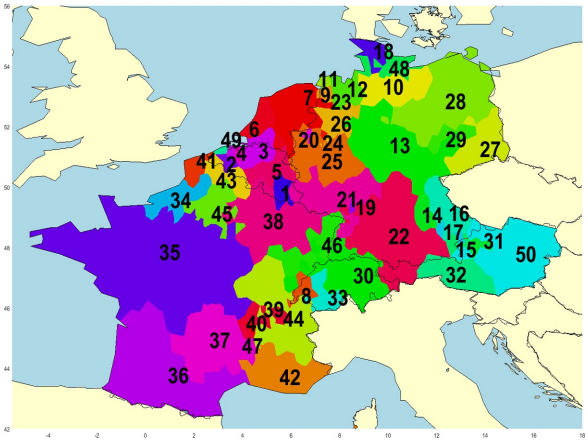

Figure 8: 50-ImpC.

One immediate observation is that - except for large parts of French borders - national borders do not align with improved PZ delimitations. Notably, the German-Austrian PZ splits apart and new PZs in Eastern Austria and Northern Germany emerge already in the 5-ImpC.

4.2. Reference Case

The impacts of these altered PZCs on overall system costs, i.e. market results and RD, are presented in fig. 9. Therein, the change in annual MCC and RDC are shown. The quantities are always compared to the BAU-C. The sum of both values is labelled system cost (SC) increase/decrease and is also given in fig. 9. SC decreases correspond to short-term welfare increases which result from improved PZCs.

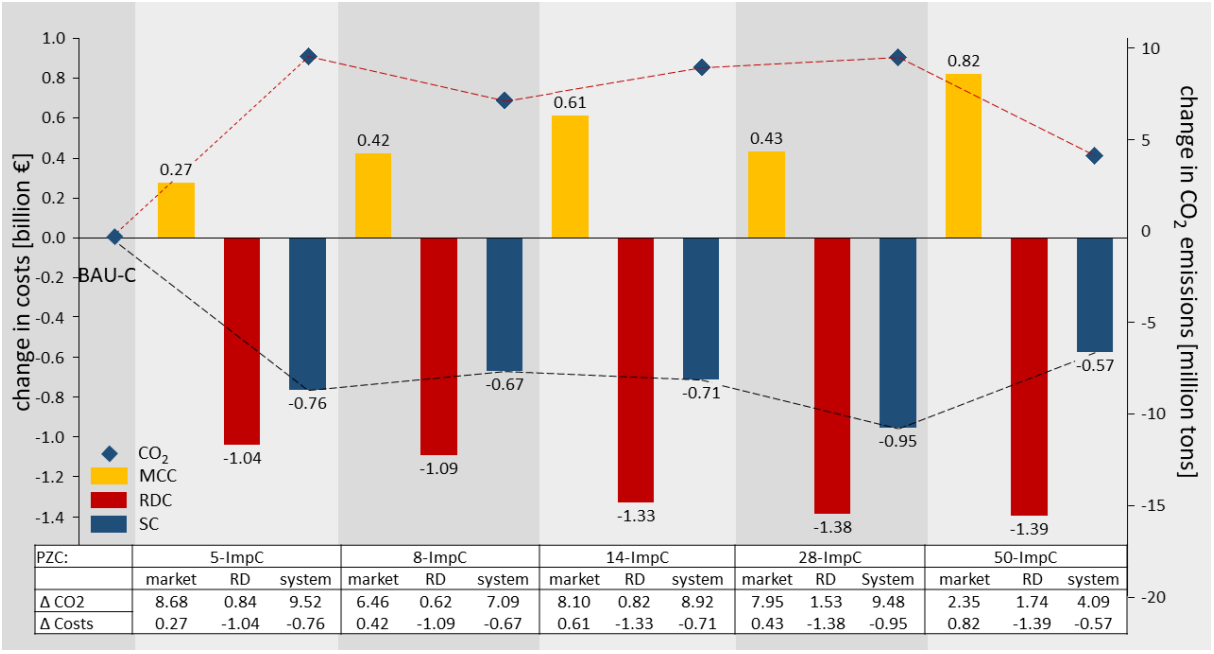

PZC:	5-ImpC			8-ImpC			14-ImpC			28-ImpC			50-ImpC		
	market	RD	system	market	RD	system	market	RD	system	market	RD	System	market	RD	system
Δ CO2	8.68	0.84	9.52	6.46	0.62	7.09	8.10	0.82	8.92	7.95	1.53	9.48	2.35	1.74	4.09
Δ Costs	0.27	-1.04	-0.76	0.42	-1.09	-0.67	0.61	-1.33	-0.71	0.43	-1.38	-0.95	0.82	-1.39	-0.57

Figure 9: Differences of MCC, RDC and SC as well as CO_2 emissions compared to BAU-C.

All improved configurations achieve lower SC than the BAU-C. The savings are mainly achieved by monotonically decreasing RDC. On the other hand, MCC are mostly higher than in the BAU-C. Yet, no clear trend is observable for MCC with increasing number of PZs. Both effects (MCC and RDC changes) add up to a non-monotonic decrease in SC with an increasing number of zones (dashed black line in fig. 9). This non-monotonicity is further discussed in sec. 4.2.4. In terms of CO_2 emissions, all assessed improved PZCs lead to emission increases. However, this is not very surprising. In our case study (as well as in the actual European certificate market), CO_2 prices are much below the level which would make electricity generation from hard coal and lignite be more expensive than gas-based generation. As MC is performed with the aim of welfare maximization, improved PZCs induce higher quantities of low-cost generation, even though the corresponding emissions are higher. However, this is a problem of pricing CO_2, not one of the investigated PZCs. As the highest SC decreases are achieved in the 28-ImpC, we focus our subsequent assessments on this configuration contrasting it with results of the BAU-C.

4.2.1. Market Results

Fig. 10 shows the yearly generation by fuel in CWE+ and selected (electrically) neighbouring countries for the BAU-C. Fig. 11 compares the generation in 28-ImpC to the BAU-C. It shows the corresponding differences in yearly electricity generation by fuel for the same countries as considered in fig. 10. The main differences are linked to the creation of smaller zones

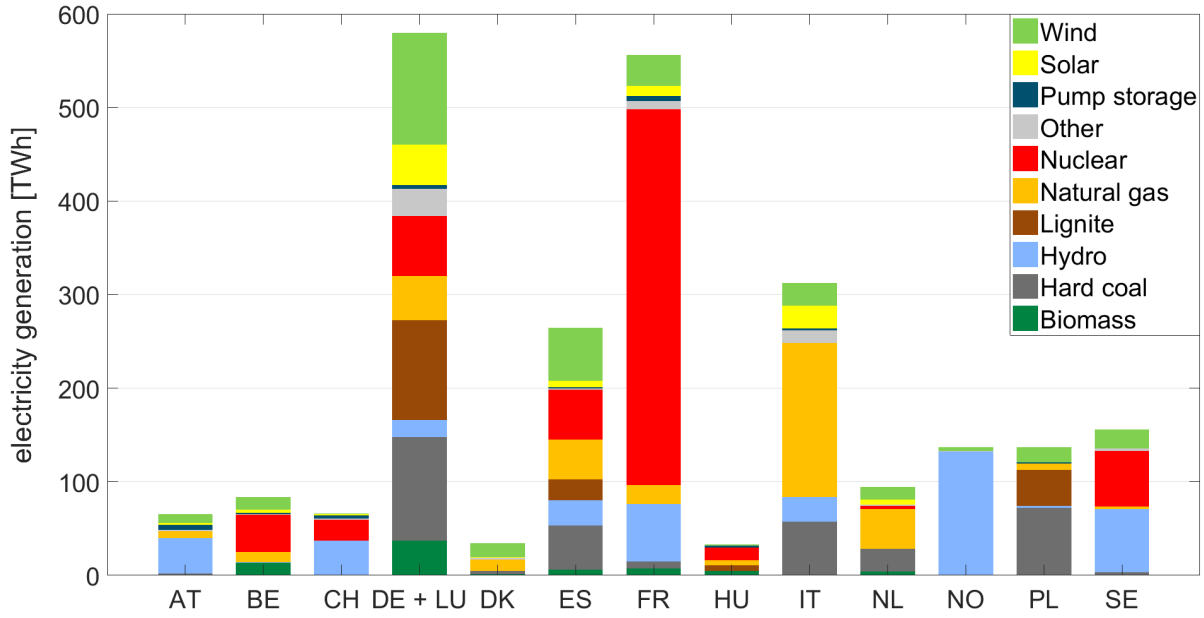

Figure 10: Electricity generation by fuel for CWE and selected (electrically) neighbouring countries for the BAU-C

in Northern Germany (cf. fig. 5 to 8). This entails that the market clearing considers LFCs inside Germany. These LFCs frequently become binding. The reason is that there is a surplus of electricity generation from wind farms in Northern Germany. Transmitting the complete surplus electricity to load centres elsewhere (load centres are mainly located in the South) increases line loadings on these inner-German lines. Thus, these LFCs frequently induce market outcomes with reduced wind-based generation from these wind farms, due to limited line transmission capacities. Generation from wind in Germany therefore decreases by around 5 TWh in the 28-ImpC. Generation from wind in Denmark is affected in a similar way (i.e. a decrease of 0.5 TWh) albeit indirectly as part of it would be transmitted through Northern Germany to the Southern regions. Similarly, Norwegian and Swedish generation from hydro reservoirs is reduced substantially (by around 5 TWh and 1 TWh respectively). These (and some other) generation reductions in the Nordic regions are mainly compensated by coal-based generation in Germany and Poland and by generation from natural gas in various Central and Southern European countries. Out of the latter group of countries, only the fossil-fuel-based generation of the Netherlands is reduced in the 28-ImpC. Considering these shifts in generation, makes the increase of CO_2 emissions in the 28-ImpC become apparent. Finally, as the market clearing induces that less generation from wind in Northern Germany and Denmark is integrated, exchanges to the

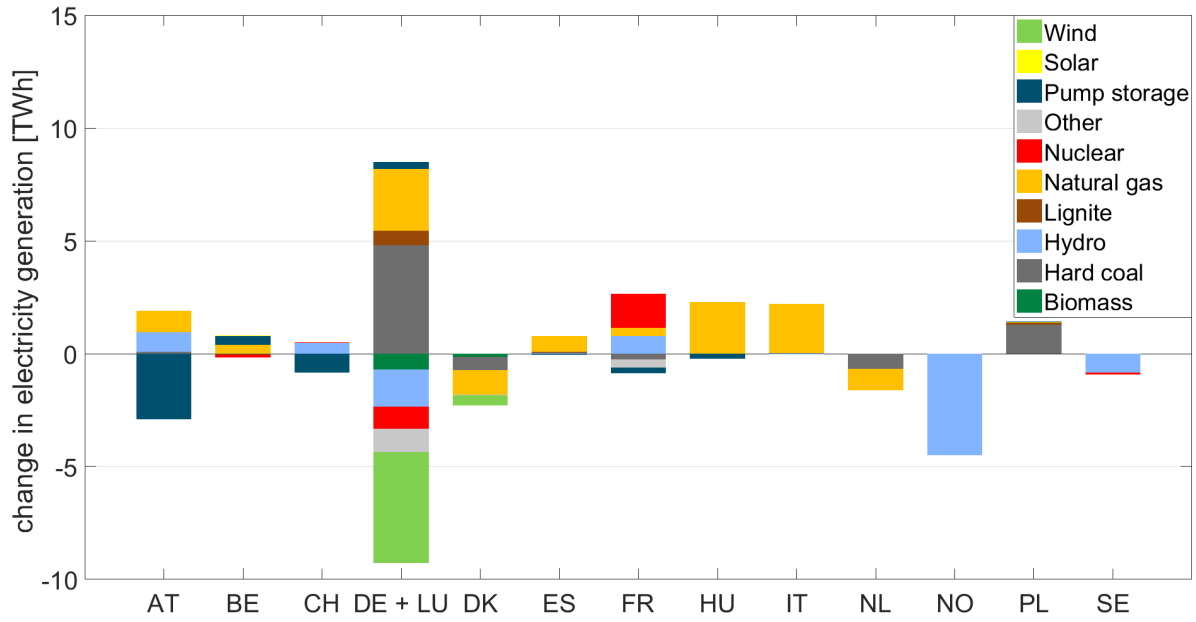

Figure 11: Change in electricity generation by fuel for CWE and selected (electrically) neighbouring countries (28-ImpC minus BAU-C)

South are also reduced. Less varying wind-based generation is scheduled to be used in the Austrian PZ, and Austrian electricity prices become less volatile. This leads to a reduced use of pump storages in Austria (approx. 3 TWh less), as this technology exploits temporal price spreads.

Table 2 shows the average electricity prices for the BAU-C and 28-ImpC.[8] As the consideration of LFCs of inner-German lines has a major impact on generation, we also provide average prices for sub-regions of Germany (North/South). One can observe increases of electricity prices in Austria, Belgium, France and Southern Germany (PZs 8, 10 and 13, cf. fig. 7), a slight decrease in Switzerland and in the Netherlands as well as a strong decrease in Northern Germany. The

Table 2: Average prices in CWE+ for the BAU-C and 28-ImpC.

prices [/MWh]	AT	BE	CH	DE	DE-North [5-7,11,26]	DE-South [8,10,12-15]	FR	NL
BAU-C	27.5	28.7	30.0	27.5	27.5	27.5	27.5	31.3
28-ImpC	33.8	30.4	30.1	27.1	18.7	29.2	28.8	30.8

smaller zones in Northern Germany (zones 6, 7, 11 and 26) even show average prices near or below zero. This plunge of prices is the consequence of a market clearing algorithm that includes transmission restrictions limiting low-cost generation in Northern Germany and in the Northern countries. If some of this generation is not eligible on the day-ahead market, a low-lost generator (e.g. a wind farm) will be the marginal generator which sets the electricity price in the corresponding PZ. In Germany, support schemes for generation from wind are in place, i.e.

[8] Where PZs and countries do not coincide (28-ImpC), prices per country are calculated as the average prices of all assigned nodes, weighted by the yearly nodal demand. Thereby, the average price per node is equivalent to the average price of the corresponding zone.

wind farm owners receive a market premium in addition to the wholesale market price for each unit of electricity generated. Thus, the marginal costs of generation from wind are even negative (in Germany) and so are the electricity prices if a wind farm is the marginal generator. In the BAU-C, wind farms do not become the marginal generator as the MC takes place as if there were no inner-German bottlenecks.[9] In terms of costs, free or very low-cost generation from wind, hydro and nuclear sources is replaced by more costly coal- and natural-gas-based generation. Hence, it is an obvious consequence that MCC increase by approx. 430 million (cf. fig. 9). Increased MCC are observed for all improved PZCs (cf. fig. 9). For 5-ImpC, the increase reaches 274 million and, then, it varies between 420 and 820 million for higher numbers of zones. This trend of increasing MCC can also be observed in [Burstedde 2012]. However, MCC changes are generally smaller and the increase is strictly monotonic. One explanatory factor for this is the difference in MC mechanisms used by [Burstedde 2012] and by us. Instead of FBMC, [Burstedde 2012] assumes an MC mechanism that considers an adjusted DC load flow without intra-zonal LFCs and aggregated nodes. Moreover, differences of input data and data aggregation (e.g. 79 aggregated grid nodes in [Burstedde 2012]) are further explanatory factors. In addition to [Burstedde 2012], our results can be contrasted with those of [Neuhoff et al. 2013]. Again, this paper is not 100% comparable to ours, as it uses NTC-based MC, considers a limited number of time steps, uses different data assumptions and only contrasts the BAU-C to nodal pricing – to name only few examples. However, [Neuhoff et al. 2013] assess SC savings to range between 0.8 to 2.0 billion . Our results are well within that range. In general, the increase of MCC with more PZs can be explained by the higher number of considered LFCs or, in the case of 5-ImpC, more relevant LFCs in the market clearing. In the BAU-C, the market clearing also considers LFCs of lines which are technically less critical (in terms of line overloads) and excludes others whose line loadings are more frequently critical. That is why, in the market clearing process, the use of low-cost generation in the BAU-C is not restricted to the same extent as in the improved configurations (which have been designed to consider the most critical lines in the MC). In principle, the impact is comparable to the previously mentioned case of market-driven wind curtailment in Northern Germany. As stated above, the MCC do not increase monotonically. We investigate this matter in detail in sec. 4.2.4.

4.2.2. Redispatch Results

In fig. 9, we have shown that RDC are decreasing monotonically. In this section, we focus on the RD amounts being the main reason for this decrease. Annual amounts are presented in table 3. For the 5-ImpC (i.e. same number of zones as in the BAU-C), the RDC decrease significantly (by 1.04 billion). As stated in sec. 2.6, the RDC vary with calibration of γ_u used in the RD assessment. In app. A, an approximation of effects is given. In particular, using $\gamma_u = 0$ could decrease the savings by around 200 million € for 28-ImpC. In turn, the choice of γ has

[9] Note that - physically - bottlenecks also exist in the BAU-C. However, they are only resolved at the redispatch stage (cf. sec. 4.2.2).

only limited effect on RD quantities. The decreasing RDCs always go along with a substantial decrease in RD quantities (approx. 13 TWh). When the PZs are broken down further, the RD amounts and RDC continue to decrease. However, the absolute decrease of these values is much less than from the BAU-C to the 5-ImpC. E.g. from 28 to 50 zones, only decreases of approx. 10 million and 0.1 TWh are achieved. The reason is that the main part of line overloads, especially on intra-zonal lines, is already avoided by the market clearing in 5-ImpC. Hence, PZs are delimited in a way that the most relevant, frequently congested lines run across zonal borders and, thus, congestion on these lines is managed more effectively. In 50-ImpC, even 97% of intra-zonal overloads compared to BAU-C can be avoided. On inter-zonal lines, overloads even increase in 5-ImpC while decreasing thereafter. Fig. 12 illustrates the improvements between

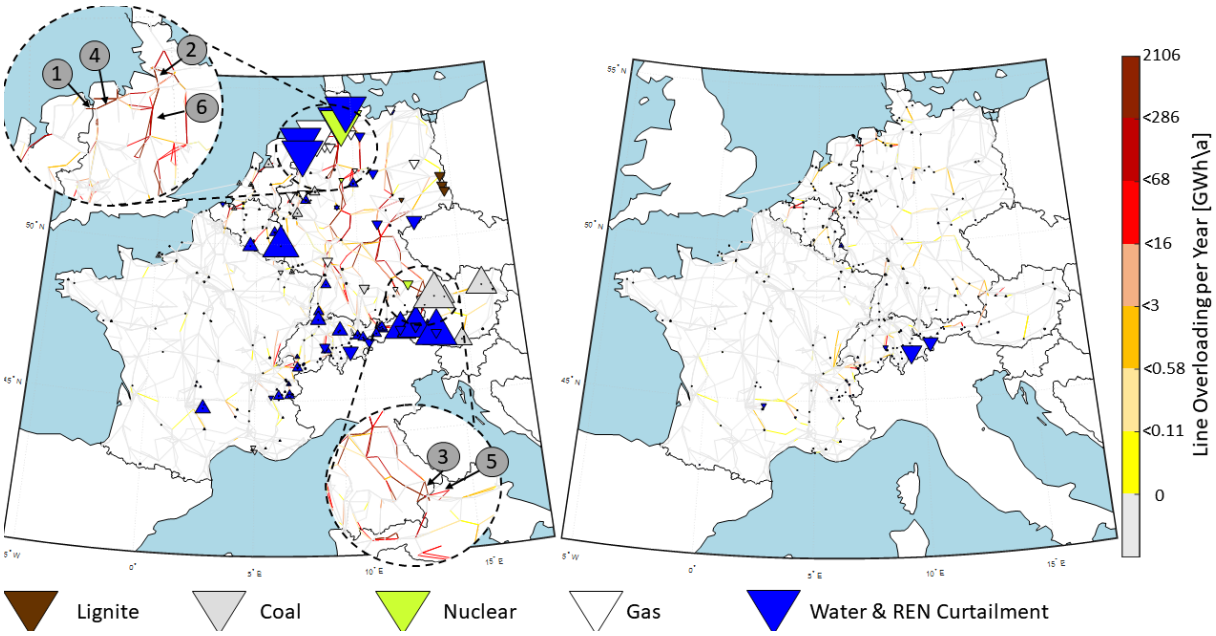

Figure 12: Redispatch amounts and yearly line overloading in BAU-C (left) and 28-ImpC (right)

Table 3: RD amounts and changes in line overloads relative to BAU-C

configuration	BAU-C	5	8	14	28	50
pos. RD [TWh]	21.3	8.2	6.3	3.3	1.9	1.8
change in overloads – inter-zonal [%]		+16	-29	-61	-81	-87
change in overloads – intra-zonal [%]		-79	-85	-93	-95	-97

the BAU-C and 28-ImpC while fig. 13 confirms the observation of a diminishing marginal benefit with an increasing number of zones. Fig. 12 presents the annual up- and down-ramping of plants and the scheduled line overloads as per market clearing. Triangles pointing upwards symbolize up-ramping, i.e. positive RD, triangles pointing downwards correspond to negative RD. The sizes of the triangles relate to the annual amounts of RD. The map on the left visualizes RD of the BAU-C while the right map in fig. 12 presents the results of the 28-ImpC. In addition, the numbers one to six indicate the position of the six most overloaded lines in the BAU-C (listed in table 4). The colors of the lines indicate the cumulated line overloads as per market clearing

throughout the year. In the BAU-C, most (scheduled) overloads occur in Northern Germany

Table 4: Overview of most congested lines in BAU-C

line	connected locations	line overloading [GWh/a] in BAU-C	considered as LFC in
1	Diele-Meeden	2,108	BAU-C, All ImpC
2	Willster-Dollern	1,802	All ImpC
3	Pleitning-Pirach	1,695	All ImpC
4	Conneforde-Diele	1,399	50-ImpC
5	Pirach-St.Peter	1,337	28-ImpC,50-ImpC
6	Sottrum-Lande	1,184	28-ImpC,50-ImpC

and at the border between Germany and Austria. Overloads on lines in Central Germany are less but still significant. In fact, four of the six most congested lines are found in Northern Germany. The other two lines are located at the border to Austria. The details are shown in the zooming circles in fig. 12 and table 4. These overloads cause the need for significant negative RD actions and curtailment of renewables in the North and North-East of Germany and positive RD in the Southern regions (mainly in Austria). The massive drop of RD, not only from the BAU-C to 28-ImpC but especially from the BAU-C to 5-ImpC, is achieved by considering the LFCs of the most congested lines in the market clearing process. Table 4 shows the configurations in which these lines are considered in the market clearing problem. The three most congested lines are explicitly considered in the 5-ImpC and are hence also present as LFCs in the other improved configurations (due to the hierarchical structure of the algorithm). The resulting effect is exhibited in fig. 13. It shows the relative changes in cumulated yearly (scheduled) line overloads compared to and normalized by the overloads of the BAU-C. The line overloads of all six lines are reduced drastically (mostly, by more than 50% by the 5-ImpC and by more than 90% latest by the 28-ImpC). Notably, the transmission line "Diele-Meeden" runs across the border between Germany and the Netherlands and, thus, is already considered in the BAU-C. However, overloads can be reduced substantially by improved PZCs (e.g. already by 30% in the 5-ImpC). By introducing the new PZs in Northern Germany, zonal line load sensitivities for FBMC are more accurate. That is, in the BAU-C, the line loading impact of infeed of wind parks is dispersed in the whole net position of the German-Austrian PZ. The new Northern German PZs are relatively small and their zonal line load sensitivities yield loads more close to the actual line loads. In addition, the relief on "Diele-Meeden" in the 5-ImpC is also due to the consideration of the LFCs of the line "Wilster-Dollern" closeby. Another important line is "Pleitning-Pirach" which runs across the German-Austrian border and whose overloads are reduced by 62% and more.[10]

[10]Note that we have assumed a common German-Austrian PZ in the BAU-C.

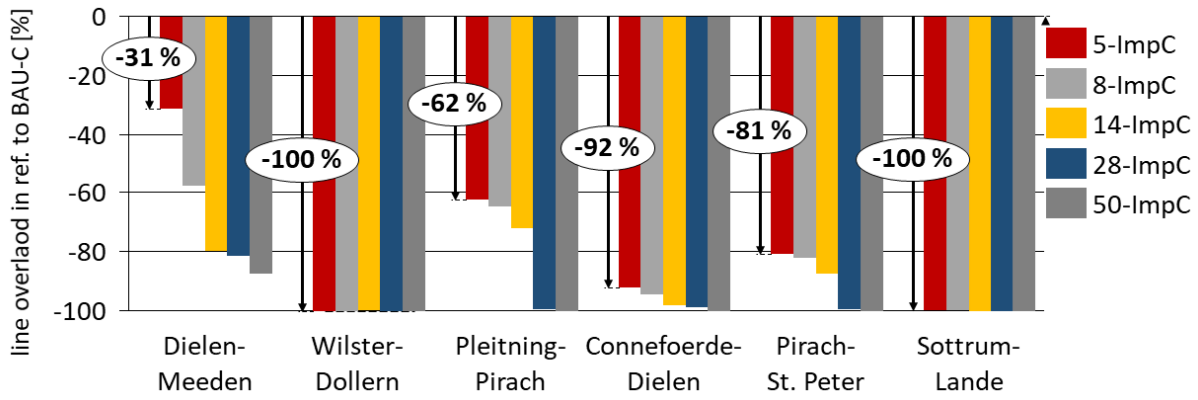

Figure 13: Reduced line overloading most congested lines in the BAU-C.

4.2.3. Distribution of Welfare Gains

Changes in MCC are composed of the negative sum of changes in consumer rents, congestion rents and producer rents. Fig. 14 shows this segmentation along with RDC. RDC strongly decrease already for the 5-ImpC compared to the BAU-C and then marginal RDC changes converge against zero for an increasing number of zones (cf. 4.1). Congestion rents show the opposite behavior, increasing almost monotonically with the number of zones, but stabilizing at an increase of approx. 1,900 million compared to the BAU-C. Consumer rents also rise with increasing number of zones, except that they are lower for 28 than for 14 zones. Producer rents show the opposite behavior, yet their decrease is much stronger than the increase in consumer rents.

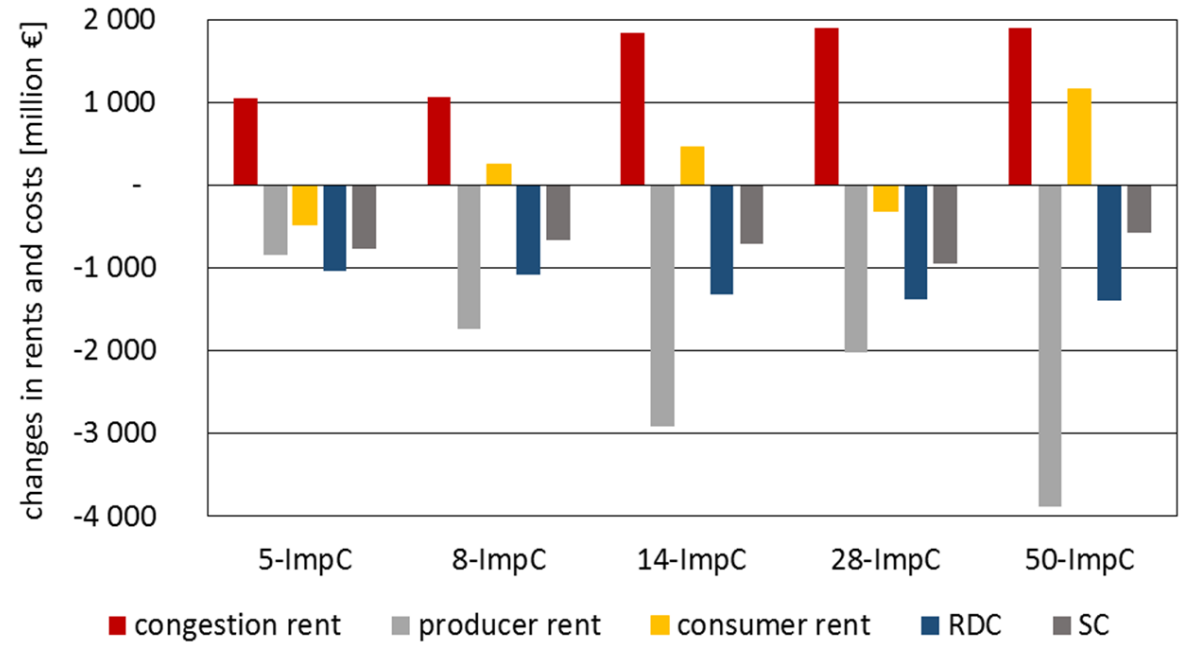

Figure 14: Changes in rents and costs compared to BAU-C for all PZCs

Additionally, changes between the 28-ImpC and the BAU-C at country level are shown in table 5. Consumer rents drop in all CWE countries except Germany and the Netherlands and increases outside CWE. This is directly related to the country-specific development of the base price (table 2). The increase in congestion rents occurs mostly in countries with a high number of significantly congested lines, i.e. in Germany and, to a lesser extent, in Belgium and France. Biggest changes in terms of producer rents occur in Germany, France and outside of CWE. In Germany and outside CWE, producer rents drop, mainly because larger amounts of low-cost wind, nuclear (Germany) and hydro (Norway) energy are replaced by more expensive fuels or generation in other countries, while prices decrease at the same time. In France, both prices and generation increase, resulting in an increased producer rent. As a result, MCC (adjusted for value of imports and exports) increase mostly in Germany and decrease especially in the Netherlands.
With RD being reduced mostly in Germany and Austria, all CWE countries except Belgium benefit in total from the PZ reconfiguration. Biggest profiteer are the Netherlands, followed by Germany and France.

Table 5: Changes in rents/costs of 28-ImpC compared to BAU-C [million]

country	cons. rent	cong. rent	prod. rent	MCC	RDC	SC
AT	-419	102	300	16	-138	-122
BE	-139	241	-259	157	-21	136
CH	-48	95	-35	-11	-12	-23
DE	255	1,228	-2,298	815	-1,172	-357
FR	-691	193	692	-194	-7	-201
LU	-14	-16	52	-22	-	-22
NL	58	13	328	-399	-31	-430
CWE	-999	1,856	-1,220	362	-1,382	-1,020
Non-CWE	685	47	-800	68	-	68
System total	-314	1,903	-2,019	430	-1,382	-952

4.2.4. Non-monotonic Rise of Market Clearing Costs

In sec. 4.2/fig. 9, we have observed that MCC do not rise monotonically. This is non-intuitive, as one would expect MCC to rise with each added LFC. The intuition may be expressed formally by stating that, for any $f(\mathbf{q}) : \mathbb{R}^n \to \mathbb{R}$, $\min_{\mathbf{q}\in Q_1} f(\mathbf{q}) \geq \min_{\mathbf{q}\in Q_2} f(\mathbf{q})$ if $Q_1 \subset Q_2$. Therein, Q_1 and Q_2 are the sets of possible solutions, i.e. equivalent to the feasible region of the electricity market clearing problems (EMCPs) for PZC_1 and PZC_2. $Q_1 \subset Q_2$ is not necessarily the case if we consider PZC_1 has more price zones than PZC_2. Basically, this can already be concluded from the analyses in Part I [Felten et al. 2019]. In conjunction with the case study, four factors may yet be highlighted:

1. Degrees of freedom: Any additional PZ z increases the degrees of freedom of the EMCP. As shown in [Felten et al. 2019], the choice of GSKs and of the base case defines a hyperplane

through the nodal feasibility polyhedron. Thus, in this regard, the feasible region of the EMCP with more PZs tends to increase (i.e. influence towards $Q_1 \supset Q_2$). This is important for managing congestion on inter-zonal and intra-zonal lines (cf. [Felten et al. 2019]).

2. Number of LFCs: More LFCs tend to reduce the feasible region of the EMCP (i.e. influence towards $Q_1 \supset Q_2$).

3. Inaccuracy of LFCs: LFCs as defined in FBMC are subject to inaccuracies. I.e. they may be overly restrictive or too loose. This statement equally holds for LFCs of an EMCP with more or less price zones (cf. [Felten et al. 2019]). Therefore, no clear tendency towards an increasing or decreasing set of possible solutions is given a priori. However, this aspect may enhance the effect of new LFCs (item 2).[11]

All four points are observable in our case study. The effects under item (1) can be found at the transition from 14-ImpC to 28-ImpC. In 14-ImpC, the Northern German PZ 3 is dominated by wind generation. The most frequently binding LFC in the EMCP of 14-ImpC is the line "Sottrum-Blockland" presented in fig. 15. PZ 3 has a zonal PTDF value of approx. 0.259 and, thereby, the highest line load sensitivity of all PZs on that line. In 28-ImpC, the PZ is split into two subzones. The new subzones 6 and 7 have the PTDFs 0.098 and 0.262 respectively. The split of PZ 3 (14-ImpC) into these two PZs yields one more degree of freedom in the EMCP. Thus, the EMCP considers that subzone 6 compounds to the congestion of this line much less than subzone 7. Therefore, the optimizer prefers infeed from subzone 6, and more wind energy can be integrated. In this region alone, approx. 0.6 TWh of additional wind energy is scheduled in the EMCP. Assuming the replacement of gas-based generation, this yields a cost reduction of around 40 million . In order to show that the changed infeed has very little influence on line loadings, we plot a line ocerload histogram for the 4,861 time stamps where the LFC of line "Sottrum-Blockland" is binding in 14-ImpC (cf. fig. 16). Scheduled overloads are even reduced by approx. 22%, while integrating more wind generation.
The impact (ii) of more LFCs in the EMCP can be seen in 50-ImpC. In this configuration, PZ 13 has two major centers of generation capacities (cf. 50-ImpC in fig. 17). A large nuclear power plant is located in the north of PZ 13 surrounded by two coal-based power plants. Towards the eastern part of the zone, there is a lignite-based generation unit. And further towards the center of PZ13, there are 2 pumped storage power plants. PZ 13 has emerged from a bigger zone (PZ 8 in 28-ImpC). Furthermore, its neighboring zones to the west, are also more fragmented than in 28-ImpC. Therefore, several new lines/LFCs are considered in the vicinity of PZ13 (cf. fig. 17).

[11] These inaccuracies may partly also be artefacts of the hierarchical cluster algorithm in conjunction with FBMC. Given its hierarchical structure, the identified solutions are close to optimal but not necessarily optimal PZCs with respect to the minimization of intrazonal LMP variation. [Felling and Weber 2018] give an intuitive example on a 4-node network that underlines this context. Moreover, the PZCs are based on LMPs. I.e. FBMC-style LFCs are not taken into account in the cluster algorithm and, thus, optimality in a FBMC environment cannot be guaranteed. However, Entso-E's methods for endogenous PZCs determination [Entso-E 2018a] do not take into account FBMC-style LFCs either.

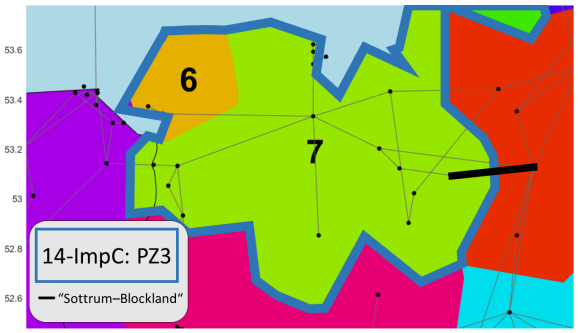

Figure 15: North DE: 14-ImpC PZ3 / 28-ImpC PZ 6 and PZ 7

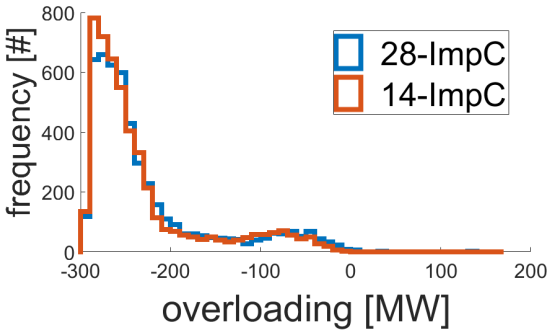

Figure 16: Overloads when binding in EMCP of 14-ImpC

Regarding impact (iii), the zonal PTDFs of PZ 13 are especially inaccurate for the lines in the east (connecting PZ 27 and PZ 29) and for the line parallel to its western delineation (connecting PZ 21 and PZ 25) in 50-ImpC. This is a consequence of using a weighted average of zonal PTDFs (cf. [Felten et al. 2019]). Also the line loads approximated by the FBMC approach are in particular inaccurate for the LFCs near PZ 13. This is seen in fig. 18. Negative overloads are equivalent to underutilization of lines, i.e. LFCs are unnecessary restrictive. When the LFCs in the vicinity of PZ 13 are binding in 50-ImpC, actual line utilization is significantly below full usage. In sum, the line underutilization is 637 GWh. Exploiting these free line capacities would improve market outcomes without entailing RD. Using the FBMC approach, net exports from PZ 13 are seen to aggravate the load situation of these lines and generation in PZ 13 is decreased - beyond what would be necessary. Therefore, only in PZ 13, PZ 27 and PZ 29, which had been one united zone in 28-ImpC, lignite-based generation decreases by around 2.4 TWh compared to 28-ImpC and coal-based generation decreases by around 1 TWh. This corresponds to MCC increases of around 180 million (assuming substitution by gas-based generation).

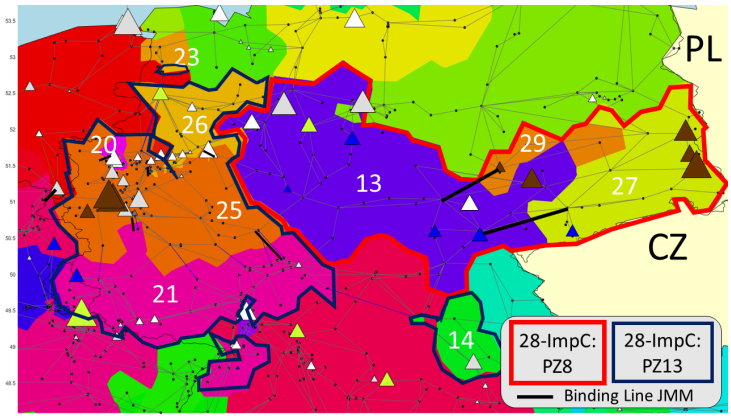

Figure 17: DE East / West 50-ImpC

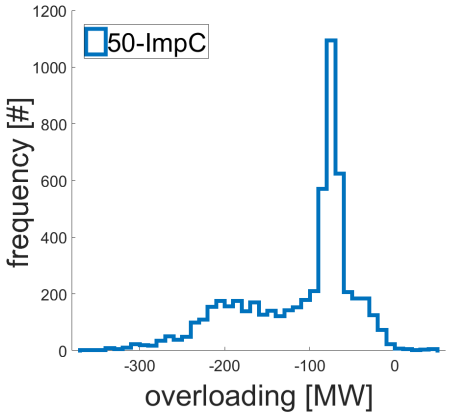

Figure 18: Overloads of lines close to PZ 13 (50-ImpC) when binding in EMCP.

In conclusion, we have shown that monotonically rising MCC cannot be expected. This is a consequence of the inaccuracies inherent to FBMC procedures (cf. [Felten et al. 2019]) in combination with price zones derived by means of a hierarchical clustering algorithm. This

result is quite specific to FBMC and shows the importance of profound model-based assessments before deciding for a new PZC out of a variety of PZC options. Under different MC mechanisms, MCC may increase monotonically and SC may decrease monotonically (cf. [Burstedde 2012]).

4.3. Results of Sensitivity Analyses

In sec. 2.3, we have explained several sensitivity analyses. Fig. 19 shows the system cost (SC=MCC+RDC) difference of the sensitivity calculations compared to the corresponding PZC run of the reference case. Overall, our data show that the results of improved PZCs are quite robust against changes in the FBMC process. I.e. the maximum SC difference occurs for 50-ImpC of the FRM Sensitivity, being 103 million . Compared to 574 million of savings in the reference case, this variation is quite small. Thus, re-classifying most congested intra-zonal lines and making them become inter-zonal has more leverage than all assessed sensitivities.

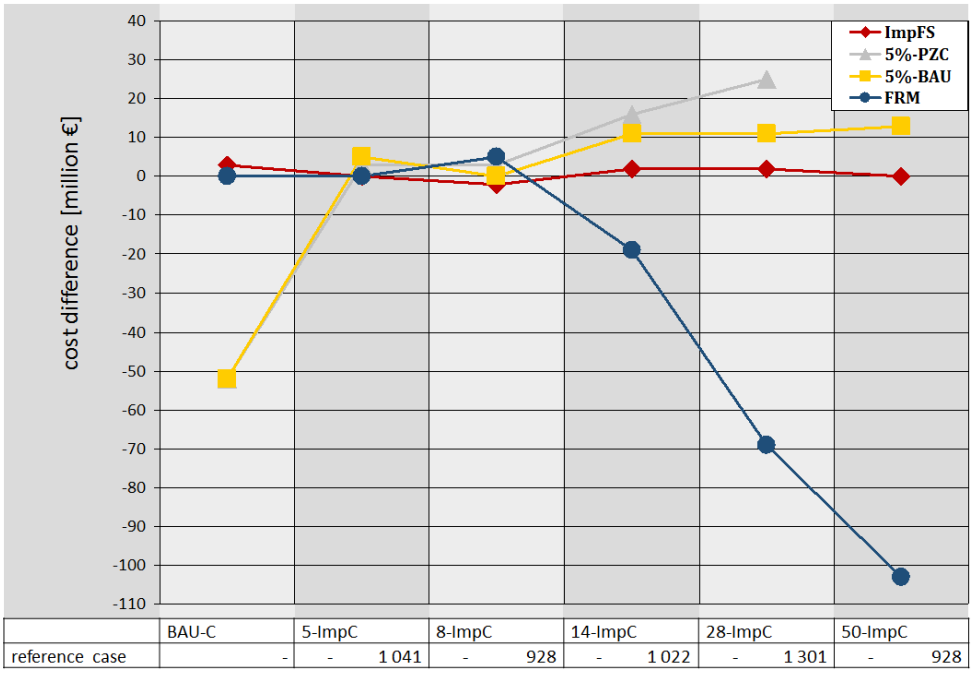

	BAU-C	5-ImpC	8-ImpC	14-ImpC	28-ImpC	50-ImpC
reference case	-	- 1 041	- 928	- 1 022	- 1 301	- 928

Figure 19: SC differences of the sensitivity calculations in comparison to the corresponding PZC reference case

Calculating FBMC parameters based on renewable time series subject to forecast errors (ImpFS) has very little influence on system costs. This result is surprising at first sight. However, the direction of a forecast error of renewables can reinforce or relieve congestion. Thus, a random and limited error seems to have no structural effect on MC results. Considering intra-zonal lines as LFCs in the EMCP (5%-PZC and 5%-BAU) leads to lower SC for the BAU-C but to increased SC especially for 14-ImpC to 50-ImpC. Considering LFCs of very rarely congested intra-zonal lines in the EMCP can only avoid little overloads. In turn, managing congestion of these lines is especially ineffective (cf. [Felten et al. 2019]). If these LFCs are inaccurate (cf. sec. 4.2.4),

it may cause welfare losses. Thus, the cost-benefit ratio of including intra-zonal LFCs becomes worse with an increasing number of PZs. The FRM sensitivity has the largest effect on SC, as it substantially lowers MCC. For 8-ImpC, the FRM decrease results in higher RD amounts and costs, even exceeding the MCC decrease. Thus, the chosen FRM decrease is too high. However, for all other PZCs, the SC decrease significantly.

5. Conclusion

In the paper at hand and its companion paper, we have presented a novel large-scale model framework that enables the reproduction of FBMC to assess power systems undergoing structural changes. We have further presented an application assessing improved PZCs in a zonal pricing regime using CWE-style FBMC. Our analysis has shown that very relevant welfare gains can be achieved by improved PZCs. Notably, RD amounts and associated costs can be reduced significantly. In the best PZC, overall welfare can be increased by around 1 billion (1.8 % of total system costs), redispatch amounts can be reduced by over 90%. While these welfare increases are very relevant, we have demonstrated that welfare gains are not equally distributed to market participants, which is likely to cause political frictions in the process of implementing improved PZCs. Furthermore, we have used the findings from Part I [Felten et al. 2019] to interpret and scrutinize our case study results. We have seen that the main driver for welfare improvements is the improved congestion management of intra-zonal lines. Nonetheless, inaccuracies inherent to the FBMC procedures gain in importance when the number of PZs is increased, while simultaneously the relevance of intra-zonal congestion diminishes. These peculiarities of FBMC should already be considered in the process of PZC determination.

References

50Hertz Transmission GmbH, Amprion GmbH, TenneT TSO GmbH, and TransnetBW GmbH (2014). *Netzentwicklungsplan Strom 2014*. Version 2014 (cit. on p. 13).

ACER (03/07/2014). *Report on the influences of existing bidding zones on electricity markets*. Ed. by ACER. URL: http://www.acer.europa.eu/official_documents/acts_of_the_agency/publication/acer%20market%20report%20on%20bidding%20zones%202014.pdf (visited on 10/13/2016) (cit. on p. 1).

Amprion, APX, Belpex, Creos, Elia, EpexSpot, RTE, Tennet, TransnetBW (2014). *Documentation of the CWE FB MC solution as basis for the formal approval-request*. Tech. rep. (cit. on p. 6).

Austrian Power Grid AG (2017). *Leitungsnetz*. URL: https://www.apg.at/de/netz/anlagen/leitungsnetz (visited on 03/23/2017) (cit. on p. 14).

BDEW Bundesverband der Energie- und Wasserwirtschaft e.V. (2017). *Redispatch in Deutschland - Auswertung und Transparenzdaten* (cit. on p. 1).

Bertsch, J., Hagspiel, S., and Just, L. (2015). *Congestion management in power systems: Long-term modeling framework and large-scale application*. Tech. rep. EWI Working Paper (cit. on p. 2).

Biggar, D. R. and Hesamzadeh, M. R. (2014). *The economics of electricity markets*. IEEE press, Wiley (cit. on p. 1).

Bjørndal, M. and Jörnsten, K. (2001). "Zonal pricing in a deregulated electricity market". In: *The Energy Journal*, pp. 51–73 (cit. on pp. 1 sq.).

Bjørndal, M. and Jörnsten, K. (2007). "Benefits from coordinating congestion management—The Nordic power market". In: *Energy policy* 35.3, pp. 1978–1991 (cit. on pp. 1 sq.).

Breuer, C. (2014). *Optimale Marktgebietszuschnitte und ihre Bewertung im europäischen Stromhandel*. deu. Hochschulschrift, Dissertation, Thesis. Zugl.: Aachen, Univ., Diss., 2014 (cit. on p. 3).

Bundesnetzagentur für Elektrizität, Gas, Telekommunikation, Post und Eisenbahnen and Bundeskartellamt (2017). *Monitoringbericht 2018* (cit. on pp. 1, 8).

Bundesnetzagentur für Elektrizität, Gas, Telekommunikation, Post und Eisenbahnen and Bundeskartellamt (2018). *Kraftwerksliste*. URL: https://www.bundesnetzagentur.de/DE/Sachgebiete/ElektrizitaetundGas/Unternehmen_Institutionen/Versorgungssicherheit/Erzeugungskapazitaeten/Kraftwerksliste/kraftwerksliste-node.html (visited on 02/22/2018) (cit. on p. 13).

Burstedde, B. (2012). "From nodal to zonal pricing: A bottom-up approach to the second-best". In: *European Energy Market (EEM), 2012 9th International Conference on the*. IEEE, pp. 1–8 (cit. on pp. 3, 20, 27).

Dierstein, C. (2017). "Impact of Generation Shift Key determination on flow based market coupling". In: *14th International Conference on the European Energy Market (EEM), Dresden* (cit. on p. 5).

Egerer, J. et al. (2015). “Two Price Zones for the German Electricity Market: Market Implications and Distributional Effects”. In: (cit. on p. 2).

Ehrenmann, A. and Smeers, Y. (2005). “Inefficiencies in European congestion management proposals”. In: *Utilities policy* 13.2, pp. 135–152 (cit. on pp. 1 sq.).

Energate GmbH (2018). *Marktdaten*. URL: `http://www.energate-messenger.de/markt/` (visited on 02/22/2018) (cit. on p. 13).

Entso-E (2015a). *Hourly load values for all countries*. URL: `https://www.entsoe.eu/db-query/consumption/mhlv-all-countries-for-a-specific-month` (cit. on p. 13).

Entso-E (2016). *Specific national considerations* (cit. on p. 13).

Entso-E (02/05/2018a). *First edition of the bidding zone review - draft version for public consultation* (cit. on pp. 1, 25).

European Commision (2015). *Commission Regulation (EU) 2015/1222 of 24 July 2015 establishing a guideline on capacity allocation and congestion management* (cit. on pp. 1 sq.).

European Network of Transmission System Operators for Electricity (Entso-E) (2015b). *Scenario Outlook And Adequacy Forecast*. Brussels. URL: `https://docs.entsoe.eu/dataset/scenario-outlook-adequacy-forecast-so-af-2015` (cit. on p. 13).

European Network of Transmission System Operators for Electricity (Entso-E) (2018b). *Transparency Platform*. Actual Generation per Production Type and Generation Forecasts for Wind and Solar. URL: `https://transparency.entsoe.eu/` (visited on 07/02/2018) (cit. on p. 6).

Felling, T. and Weber, C. (2018). “Consistent and robust delimitation of price zones under uncertainty with an application to Central Western Europe”. In: *Energy Economics* 75, pp. 583–601 (cit. on pp. 3 sqq., 25).

Felten, B. (06/20/2016). *CHP Plant Operation and Electricity Market Prices – Analytical Insights and Large-Scale Model Application*. 39th IAEE International Conference (cit. on p. 7).

Felten, B., Baginski, J. P., and Weber, C. (2017). *KWK-Mindest- und Maximaleinspeisung - Die Erzeugung von Zeitreihen für die Energiesystemmodellierung*. HEMF Working Paper No. 10/2017. URL: `https://papers.ssrn.com/sol3/papers.cfm?abstract_id=3082858` (visited on 12/11/2017) (cit. on pp. 7, 10).

Felten, B., Felling, T., Osinski, P., and Weber, C. (2019). “Flow-Based Market Coupling Revised - Part I: Analyses of Small- and Large-Scale Systems”. In: *Energy Economics* XX.X, pp. X–X (cit. on pp. 1 sq., 4–7, 11, 13, 24–27, 29).

Finck, R., Ardone, A., and Fichtner, W. (2018). “Impact of Flow-Based Market Coupling on Generator Dispatch in CEE Region”. In: *2018 15th International Conference on the European Energy Market (EEM), Lódz, PL, June 27–29, 2018*. 37.06.01; LK 01. IEEE, Piscataway, NJ, pp. 1–5 (cit. on p. 2).

Frontier Economics and Consentec (02/05/2008). *Methodische Fragen bei der Bewirtschaftung von innerdeutschen Engpässen im Übertragungsnetz (Energie)*. Untersuchung im Auftrag der Bundesnetzagentur für Elektrizität, Gas, Telekommunikation, Post und Eisenbahnen (cit. on p. 9).

Grimm, V., Kleinert, T., Liers, F., Schmidt, M., and Zöttl, G. (2017). "Optimal price zones of electricity markets: a mixed-integer multilevel model and global solution approaches". In: *Optimization Methods and Software* 34.2, pp. 406–436. eprint: https://doi.org/10.1080/10556788.2017.1401069. URL: https://doi.org/10.1080/10556788.2017.1401069 (cit. on p. 2).

Grimm, V., Martin, A., Weibelzahl, M., and Zöttl, G. (2016). "On the long run effects of market splitting: Why more price zones might decrease welfare". In: *Energy Policy* 94, pp. 453–467 (cit. on p. 2).

Hogan, W. W. (1992). "Contract networks for electric power transmission". In: *Journal of Regulatory Economics* 4.3, pp. 211–242 (cit. on p. 1).

Imran, M. et al. (12/2008). "Effectiveness of zonal congestion management in the European electricity market". In: *Power and Energy Conference, 2008. PECon 2008. IEEE 2nd International*, pp. 7–12 (cit. on p. 3).

International Energy Agency (2014). *IEA Electricity Information*. Tech. rep. (cit. on p. 13).

Kłos, M. et al. (10/2014). "The scheme of a novel methodology for zonal division based on power transfer distribution factors". In: *IECON 2014 - 40th Annual Conference of the IEEE Industrial Electronics Society*, pp. 3598–3604 (cit. on p. 3).

Löschel, A., Flues, F., Pothen, F., and Massier, P. (2013). *Den Strommarkt an die Wirklichkeit anpassen: Skizze einer neuen Marktordnung*. ZEW Discussion Paper No. 13-065 (cit. on p. 1).

Marjanovic, I., v. Stein, D., van Bracht, N., and Moser, A. (2018). "Impact of an Enlargement of the Flow Based Region in Continental Europe". In: *2018 15th International Conference on the European Energy Market (EEM)*, pp. 1–5 (cit. on p. 2).

Meibom, P. et al. (2011). "Stochastic Optimization Model to Study the Operational Impacts of High Wind Penetrations in Ireland". In: *IEEE Transactions on Power Systems* 26.3, pp. 1367–1379 (cit. on p. 7).

Meibom, P. et al. (2006). *Wilmar joint market model. Documentation*. Tech. rep. Risø National Laboratory (cit. on pp. 7, 10 sq.).

Neuhoff, K. et al. (2013). "Renewable electric energy integration: quantifying the value of design of markets for international transmission capacity". In: *Energy Economics* 40, pp. 760–772 (cit. on pp. 2, 20).

Oberlandesgericht Düsseldorf (04/28/2015). *Beschluss VI-3 Kart 313/12 (V)* (cit. on p. 9).

Oggioni, G. and Smeers, Y. (2013). "Market failures of Market Coupling and counter-trading in Europe: An illustrative model based discussion". In: *Energy Economics* 35, pp. 74–87 (cit. on pp. 1 sq.).

RTE France (2015). *Static Grid Model*. URL: https://clients.rte-france.com/lang/an/visiteurs/vie/indispos_caracteristiques_statiques.jsp (cit. on p. 14).

S & P Global Platts (2018). *World Electric Power Plants Database*. URL: https://www.platts.com/products/world-electric-power-plants-database (visited on 02/22/2018) (cit. on p. 13).

Sarfati, M. et al. (07/2015). “Five indicators for assessing bidding area configurations in zonally-priced power markets”. In: *2015 IEEE Power Energy Society General Meeting*, pp. 1–5 (cit. on p. 3).

Steffen, B. and Weber, C. (2016). “Optimal operation of pumped-hydro storage plants with continuous time-varying power prices”. In: *European Journal of Operational Research* 252.1, pp. 308–321 (cit. on p. 11).

TenneT TSO GmbH (2015). *Static Grid Model*. URL: `https://www.tennettso.de/site/en/Transparency/publications/static-grid-model/static-grid-model` (visited on 03/23/2017) (cit. on p. 14).

Trepper, K., Bucksteeg, M., and Weber, C. (2015). “Market splitting in Germany – New evidence from a three-stage numerical model of Europe”. In: *Energy Policy* 87, pp. 199–215 (cit. on pp. 2, 7).

Tuohy, A. et al. (2009). “Unit Commitment for Systems With Significant Wind Penetration”. In: *IEEE Transactions on Power Systems* 24.2, pp. 592–601 (cit. on p. 7).

Van den Bergh, K. et al. (04/2016). “The impact of bidding zone configurations on electricity market outcomes”. In: *2016 IEEE International Energy Conference (ENERGYCON)*, pp. 1–6 (cit. on p. 3).

Wyrwoll, L., Kollenda, K., Müller, C., and Schnettler, A. (2018). “Impact of Flow-Based Market Coupling Parameters on European Electricity Markets”. In: *2018 53rd International Universities Power Engineering Conference (UPEC)*, pp. 1–6 (cit. on p. 2).

Zimmermann, R., Murillo-Sánchez, C., and Thomas, R. (2011). “MATPOWER: Steady-State Operations, Planning and Analysis Tools for Power System Research and Education”. In: *IEEE Transactions on Power Systems* 26.1, pp. 12–19 (cit. on pp. 5, 9 sq.).

Appendix

A. Redispatch Sensitivity

In sec. 2.5.1 we have introduced the factor γ_u. Table 6 presents the corresponding RDCs and amounts for different γ_u values between 0 and 0.3. Results show that the amounts of redispatch

Table 6: Sensitivity results for the factor γ_u in the BAU-C.

γ_u	0	0.1	0.2	0.3
pos. RD [TWh]	22.11	21.92	21.81	21.93
RDC [million EUR]	1,200	1,302	1,404	1,517
Δ RDC to $\gamma_u = 0.2$ [million EUR]	-204	-102	-	+113

do not vary significantly for different values of γ_u. The absolute difference between the maximum and minimum value is around 186 GWh, which corresponds to less than 1% of the RD amounts. Yet, regarding costs, there is a substantial difference. In absolute terms, RDC increase about 300 million € comparing the RDCs for $\gamma_u = 0$ and $\gamma_u = 0.3$. In relative terms, this constitutes an increase of about 21%.

Table 7 presents how the SC savings depend on the choice of γ_u for the different PZCs. We present the SC changes (ΔSC) calculated with the γ_u chosen in our case study (=0.2) and with the lower bound value ($\gamma_u = 0$). Thus, $\gamma_u = 0$ constitutes a worst-case approximation of the system cost savings. Obviously, RDCs calculated with $\gamma_u = 0$ are always lower than those calculated with $\gamma_u = 0.2$. In case of the 28-ImpC, the SC savings compared to the BAU-C would decrease from 948 million € to 744 million € (i.e. decreasing by 22%). Thus, one should be aware of the dependency on γ_u. However, the worst-case approximation yields savings of 744 million €, which still represents a very significant amount.

Table 7: Change in system costs (SC_{X-ImpC} - SC_{BAU}) calculated with $\gamma_u = 0.2$ and $\gamma_u = 0$.

PZC (x-ImpC with $\gamma_u = 0.2$)	5-ImpC	8-ImpC	14-ImpC	28-ImpC	50-ImpC
ΔSC for $\gamma_u = 0.2$	-0.76	-0.67	-0.71	-0.95	-0.57
ΔSC for $\gamma_u = 0$ in BAU-C	-0.56	-0.47	-0.51	-0.75	-0.37

Acknowledgements

This research has partly been funded by the Federal Ministry of Economics and Technology (BMWi) of Germany within the framework of the joint project “KoNeMaSim – Kopplung von Netz- und Marktsimulationen für die Netzplanung” (project number 03ET7526). The authors gratefully acknowledge the financial support.

Correspondence

Tim Felling
Research Associate
House of Energy Markets and Finance
University of Duisburg-Essen, Germany
Universitätsstr. 12, 45117 Essen
Tel. +49 201 183-6706
Fax. +49 201 183-2703
E-Mail tim.felling@uni-due.de

Björn Felten
Research Associate
House of Energy Markets and Finance
University of Duisburg-Essen, Germany
Universitätsstr. 12, 45117 Essen
Tel. +49 201 183-3389
Fax. +49 201 183-2703
E-Mail bjoern.felten@uni-due.de

Paul Osinski
(Corresponding Author)
Research Associate
House of Energy Markets and Finance
University of Duisburg-Essen, Germany
Universitätsstr. 12, 45117 Essen
Tel. +49 201 183-6713
Fax. +49 201 183-2703
E-Mail paul.osinski@uni-due.de

Prof. Dr. Christoph Weber
Teaching Professor
House of Energy Markets and Finance
University of Duisburg-Essen, Germany
Universitätsstr. 12, 45117 Essen
E-Mail christoph.weber@uni-due.de